*Pathology International* 2005; **55**: 753–756

Rapid Communication

# Simultaneous imaging of membrane antigen and the corresponding chromosomal locus in pathology archives

**Hisaki Igarashi,[1] Kimihiro Yamashita,[1] Masaya Suzuki,[1] Yasuhiko Kitayama,[1,2] Jun Isogaki,[3] Keiji Maruyama,[3] Ken-ichi Sunayama,[3] Hitoshi Tsuda,[4] Takachika Ozawa,[5] Shinichiro Kiyose[1] and Haruhiko Sugimura[1]**

*Departments of [1]Pathology and [3]Surgery, Hamamatsu University School of Medicine, [5]Department of Pathology, Hamamatsu Medical Center, Hamamatsu, [2]Department of Pathology, Shizuoka Saiseikai Hospital, Shizuoka and [4]Department of Pathology, National Medical Defense College, Tokorozawa, Japan*

**A new procedure for the simultaneous staining of membranous antigens, such as tyrosine kinase-type cell surface receptor HER2 (c-erbB2), and the corresponding chromosome (chromosome 17 for c-erbB2) in the same cell for use in examining pathology archives is presented. A multistep procedure involving microwave-assisted fluorescence *in situ* hybridization and immunofluorescence yielded cell images having c-erbB2 on the membrane and genomic signals from the chromosome 17 centromere and the c-erbB2 locus. Furthermore, a combination of microwave-assisted chromogenic *in situ* hybridization and immunohistochemistry found colorized signals from both chromosome 17 centromere in the nuclei and c-erbB2 on the membranes of individual cells. Quantitative image analysis further confirmed the presence of a significantly stronger c-erbB2 immunoreactivity on cells containing three or more signals from chromosome 17 than from those with less than three signals. It was possible to extend the constellation of cell surface markers and corresponding chromosomes or locus-specific makers to several other genes including CDH1. In this case, the disappearances of CDH1 expression, a CDH1 locus signal, and a centromere enumeration probe (CEP) 16 signal were simultaneously demonstrated in the less-adhesive tumor cells. Thus, it is believed that this procedure might pave the way for exploiting pathology archives for the genotype–phenotype analysis of individual cells.**

**Key words:** chromogenic *in situ* hybridization, CISH, FISH, fluorescence *in situ* hybridization, hercep test, immunohistochemistry, microwave, pathology archives

Correspondence: Haruhiko Sugimura, MD, PhD, Department of Pathology, Hamamatsu University School of Medicine, 1-20-1 Handayama, Hamamatsu 431-3192, Japan.
Email: hsugimur@hama-med.ac.jp

Received 13 July 2005. Accepted for publication 19 August 2005.

Obtaining information on membrane antigens, and the chromosomal status of the indicated cells simultaneously in pathology archives has been a challenge to many investigators for many years. Extending our recent success in the retrieval of fluorescent *in situ* hybridization (FISH) signals from chromosome centromeres in the pathology archives, which were stored as paraffin blocks at room temperature for several years,[1–7] we here developed a consecutive procedure consisting of immunostaining for membranous antigens and chromogenic *in situ* hybridization (CISH) for centromere signals.

Using this procedure, one of the membranous antigens frequently used in clinical settings, c-erbB-2, and its related chromosomal signals, were successfully visualized under an ordinary microscope. This procedure (Patent no. 2002-324433 in Japan) in combination with the currently available genome database would facilitate the identification of large-scale chromosomal change(s) and related protein expressions in the same cells in pathology archives.

## MATERIALS AND METHODS

The procedure consisted of three steps: ordinary immunostaining followed by microwave-assisted FISH and secondary immunostaining for fluoroisothiocyanate (FITC). Two different colorizations were performed using 3′,3′-diaminobenzidine (DAB) and new fuchsin, the substrates for peroxidase and alkaline phosphatase, respectively. Centromere enumeration probes (CEP) 16 and 17 (Abbott Diagnostics, formerly Vysis, Abbott Park, IL, USA) and locus-specific probes based on bacterial artificial chromosome (BAC, Advanced Geno Techs, Tsukuba, Japan) were used. Purified BAC DNA was labeled with spectrum orange or spectrum green (Abbott Diagnostics) using a nick translation

kit (Abbott Diagnostics). Various modifications including antigen retrieval methods by protease or heat could be added to the process according to the targets and fixation conditions. The following protocol is the best for the tissues fixed in 10% neutralized formalin for <48 h. The modifications of the procedures required for the tissues for longer fixations are available on request. The principles of the procedure are schematized in Fig. 1.

### CISH for *c-erbB-2*-CEP 17

A 5 μm section of breast cancer tissue was dewaxed and boiled in citrate buffer for 15 min. Alternately, there are several modifications in this step.

Any one of the following five pretreatments should be tried after dewaxing according to the antibodies.

(1) Incubate it in the antigen retrieval solution supplied in the HercepTest II (DakoCytomation, Glostrup, Copenhagen) kit for 40 min at 95–99°C.

(2) Treat with protease supplied in Histofine HER2 kit (Nichirei, Tokyo, Japan) for 5 min at room temperature.

(3) Incubate in 0.3% pepsin (DakoCytomation) for 10 min at 37°C.

(4) Treat with proteinase K (Sigma, St Lois, MO, USA) in 400 μg/mL for 5 min at room temperature.

(5) Microwave treatment in 0.01 mol/L citrate buffer, 100°C for 15 min.

When the antigens not requiring a retrieval procedure are targeted, these pretreatments were unnecessary. In the present report we used pretreatment 1.

After blocking endogenous peroxidase with 0.3% hydrogen peroxide/methanol, the tissue was incubated with a primary antibody, a rabbit polyclonal antibody to c-erbB2 oncoprotein (HER2/neu) (A0485, DakoCytomation), for 60 min and polymer colorization was performed using DAB and the Envision+ system (DakoCytomation). After confirming the membranous staining of HER2 on the cells, the section was rinsed with phosphate-buffered saline and dehydrated. When using pretreatments 1–4, the slide must be boiled in 0.01 mol/L citrate buffer for 15 min before the next step. Alternately when pretreatment 5 is used, the slide must be treated in 0.3% pepsin/0.01 N HCl for 10 min at 37°C or in proteinase K (10 μg/mL) for 5 min at room temperature. The aging procedure of pretreatment with 0.1% NP-40/2 × SSC (0.3 mol/L NaCl, 30 mmol/L Na citrate, pH 7.2) was then performed for 30 min at 37°C. The section was then denatured with 70% formamide/2 × SSC at 85°C for 10 min, followed by dehydration with cold ethanol.

The FISH procedure using intermittent microwave irradiation for the examination of pathology archives has been previously reported.[1–7] Briefly, the section was hybridized with spectrum green-labeled CEP 17 (Abbott Diagnostics) under a microwave processor (MI-77; Azumaya, Tokyo, Japan) and irradiated for 3 s on and 2 s off at 42°C for 1 h during the initial 16 h of hybridization, followed by consecutive rinsing 50%formamide/2 × SSC, 2 × SSC, 2 × SSC/0.1%NP40, and 2 × SSC. Nuclear staining was done using 4,6-diamidino-2-phenylindol (1000 ng/mL), and the FISH signals were monitored under a fluorescence microscope. The slides were then incubated with anti-FITC antibody conjugated with alkaline phosphatase (DakoCytomation) for 30 min at 42°C. Colorization was performed using a new fuchsin substrate kit (Histofine; Nichirei, Tokyo, Japan), according to the company's instructions. To identify the c-erbB2 locus, a mixture of BAC clones (RP11-62N23, RP11-94L15, RP11-387H1) was used.

### Triple staining for E-cadherin–CEP 16–*CDH1*

In this experiment, the primary antibody used was anti-E-cadherin (CDH1; monoclonal, 36B5; Novocastra, Newcastle upon Tyne, UK). Polymer colorization was performed using DAB and the Envision+ system (DakoCytomation). The autofluorescence of DAB is shown on the cell membrane in crimson in Fig. 2(c,d). A BAC clone RP11-495A4 (Advanced Geno Techs) and CEP 16 (Abbott Diagnostics) were used to detect the *CDH1* locus and centromere 16, respectively. CEP 16 had been labeled with spectrum green. A BAC clone RP11-495A4 was purified using a Large Construct kit (Qiagen, Hilden, Germany). The purified DNA was nick-translated with spectrum orange-conjugated deoxyuridine 5-triphosphate (Abbot Diagnostics) according to the company's instructions.

A schematic explanation for this stepwise procedure is shown in Fig. 1.

### Semiquantitative evaluation of the staining

#### *Validation of the software*

The numbers of CEP 17 and CEP 16 signals were counted manually, and the immunostaining results for the corresponding cells were quantitatively evaluated using Tamamushi, a new software for image analysis developed by K. Sunayama and K. Maruyama in the Second Department of Surgery, Hamamatsu University School of Medicine. The validity of this software was tested using manually scored slides for the Hercep test (Roche, available from the authors). Immunostained slides of breast cancer tissue stained with anti c-erbB2 were scored as 1+, 2+, or 3+ by an authorized pathologist (HT), and the images were captured and quantified by Tamamushi. This software can cal-

culate the mean value of the brightness of a small portion (up to $5 \times 5$ pixels) of an area and can cover a continuous area. Briefly, the captured images were digitized to image files using a microscope charge coupling device camera system (HC-2000; Olympus, Tokyo, Japan) at $2.5 \times 40$ magnification. The cells in the images were then scanned and the immunoreactivity of each cell was calculated as a density. Each image contained up to 10 cells and the immunoreactivity of each cell was evaluated. The calculated densities (white, 0; black, 1.0) for the Hercep test score categories (1+, 2+, and 3+) were significantly different.

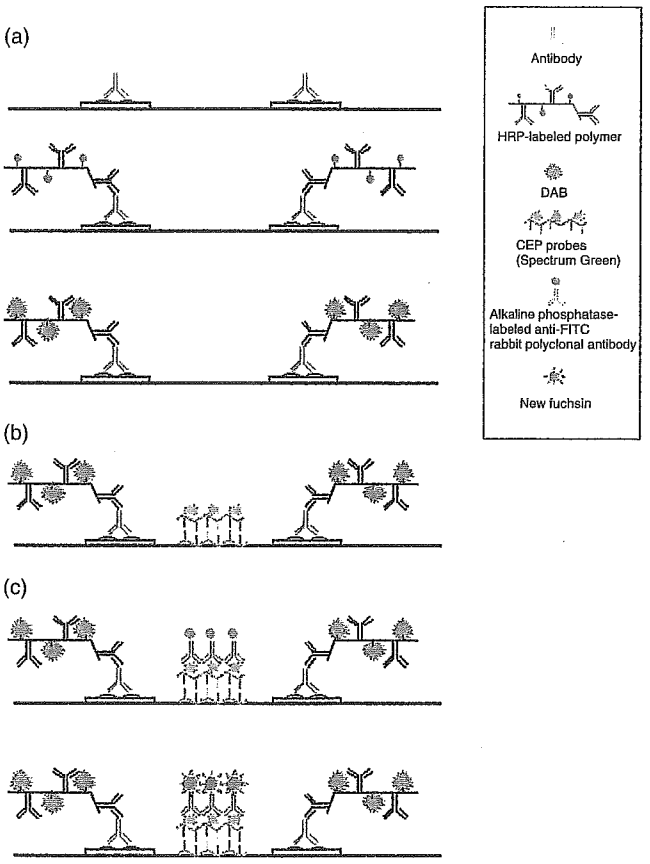


**Figure 1** Consecutive staining procedure for fluorescence *in situ* hybridization (FISH) and immunohistochemistry. (**a**) First step (immunohistochemistry). (Upper panel) Incubate with the first antibody (A0485; antihuman c-erbB-2 oncoprotein (HER2/neu), DakoCytomation) diluted 1:100 for 1 h at room temperature. (Middle panel) Incubation with the polymers using ChemMate Envision (K 5027, DakoCytomation) for 30 min at room temperature. (Lower panel) Colorization with 3-3′-diaminobenzidine (DAB; Dojin, Kumamoto, Japan) for 10 min until brown membranous immunoreactivity can be identified. (**b**) Second step (microwave-irradiated fluorescence *in situ* hybridization, MI-FISH). Green symbol represents spectrum green incorporated into the probe, which is hybridized. (**c**) The third step showing alkaline phosphatase-conjugated anti-fluoroisothiocyanate (FITC) bound to spectrum green, and colorized with new fuchsin. HRP, horseradish peroxidase; CEP, centromere enumeration probe.

*Immunoreactvity and centromere signals*

Using Tamamushi, the area of one section of each cell membrane in up to 20 cancer cells containing one, two, three, or four CEP 17 centromere signals, was scanned circumferentially, and the values of the density representing the immunoreactivity of antic-erbB2 were estimated. We divided the cells into three groups according to centromere number. The distribution of the values among the groups divided according to the centromere signal number was then evaluated. An Aspin–Welch *t*-test was performed for all combinations using the SAS program (SAS Institute, Cary, NC, USA).

## RESULTS AND COMMENTS

Concurrent imaging CISH is shown in Fig. 2(a,b). The cells with strong membranous staining of c-erbB2 have polyploidal centromeres of chromosome 17 (arrows in Fig. 2b). The

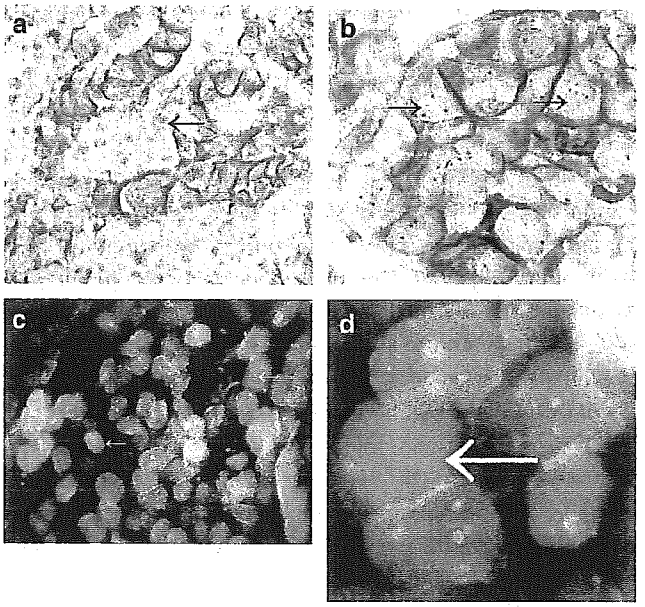


**Figure 2** (**a**) Simultaneous colorization of c-erbB2 and centromere enumeration probe (CEP) 17. The red dots represent chromosome 17 centromeres and the brown membranous immunoreactivity shows the c-erbB2 product. The heterogeneous staining of the tumor cells is visible (original magnification, ×40). The cells with two signals or less exhibit faint or no membranous staining (arrow). (**b**) Higher magnification of (**a**). An area of tumor cells with strong immunoreactivity is shown (original magnification, ×100). The cells having ≥3 signals show distinct membranous expression (arrows). (**c**) Simultaneous colorization of CDH1 and two chromosomal signals, CEP 16 and the *CDH1* locus, are shown. The consistent loss of CEP 16 and the *CDH1* locus-specific probe corresponds to the loss of both immunoreactive membranous CDH1 and cell–cell adhesion (original magnification, ×100). Most of the tumor cells attached to each other have two red and green signals with membranous staining. The cells with signal deletion look less adhesive (arrows). (**d**) Only one signal each and the absence of CDH1 expression (arrow).

**Table 1** Densities of the immunoreactivity to c-erbB2 of individual cells, meaured by Tamamushi

| | No. cells measured | Mean ± SD | *P*† vs 1 | vs 2 | vs 3 | vs 4 |
|---|---|---|---|---|---|---|
| Control (non-tumorous epithelium) | 5 | 0.364 ± 0.019 | 0.0453 | 0.024 | <0.0001 | 0.0005 |
| No. CEP 17 signals per cancer cell | | | | | | |
| 1 | 10 | 0.42 ± 0.056 | – | 0.545 | <0.0001 | 0.0006 |
| 2 | 18 | 0.403 ± 0.057 | – | – | <0.0001 | 0.0004 |
| 3 | 20 | 0.599 ± 0.057 | – | – | – | 0.1934 |
| 4 | 4 | 0.565 ± 0.039 | – | – | – | – |

†Aspin–Welch *t*-test.

cells without overexpressed membranous HER2 generally seemed to have the normal two signals. As shown in Table 1, the numbers of centromere signals and the quantified immunoreactivity of the corresponding cells were well correlated, verifying the previous data obtained by independent observations of immunostaining, FISH, and CISH.[8,9] Furthermore, our procedure revealed certain heterogeneous situations such as instances where cells with three or more signals had less membranous immunoreactivity and vice versa, implying more complicated situations in individual cancer cells (data not shown). Pathological and molecular heterogeneity are two of the major obstacles to be overcome in molecular targeted therapy.

As for E-cadherin expression, the loss of E-cadherin expression and the loss of CEP 16 were visible in the same breast cancer cells, which appeared to be separated from each other (Fig. 2c,d). The non-adhesiveness of tumor cells has usually been explained by the epigenetic downregulation of E-cadherin and/or the loss of heterozygosity,[10] thus a straightforward loss of that genome in particular cells is consistent with its loss of adhesiveness in these cells.

We believe that our method described here may pave the way for searching for the simultaneous alteration of any genomic fragment and its product in the same cell. Currently, BAC clones covering the whole human genome are available, and a proper labeling of these clones will generate a profile of cancer cell genome dosages in pathology archives. This approach may also complement extraction of DNA from dissected tissues and BAC array hybridization.

## ACKNOWLEDGMENTS

We thank Ms Kiyoko Nagura for her excellent technical assistance, and Dr Soeda for the preparation of the BAC clone. This work was supported in part by a Grant-in-Aid from the Ministry of Health, Labour and Welfare for the 2nd-term Comprehensive 10-Year Strategy for Cancer Control and from the Ministry of Education, Culture, Sports, Science (17015017) and Technology of Japan on Priority Area and the 21st century COE program 'Medical Photonics', and by the Smoking Research Foundation.

## REFERENCES

1 Kitayama Y, Igarashi H, Sugimura H. Amplification of FISH signals using intermittent microwave irradiation for analysis of chromosomal instability in gastric cancer. *Mol Pathol* 1999; **52**: 357–9.
2 Kitayama Y, Igarashi H, Sugimura H. Different vulnerability among chromosomes to numerical instability in gastric carcinogenesis: Stage-dependent analysis by FISH with the use of microwave irradiation. *Clin Cancer Res* 2000; **6**: 3139–46.
3 Kitayama Y, Igarashi H, Sugimura H. Initial intermittent microwave irradiation for fluorescence in situ hybridization analysis in paraffin-embedded tissue sections of gastrointestinal neoplasia. *Lab Invest* 2000; **80**: 779–81.
4 Kitayama Y, Igarashi H, Watanabe F, Maruyama Y, Kanamori M, Sugimura H. Nonrandom chromosomal numerical abnormality predicting prognosis of gastric cancer: A retrospective study of 51 cases using pathology archives. *Lab Invest* 2003; **83**: 1311–20.
5 Kobayashi K, Kitayama Y, Igarashi H *et al.* Intratumor heterogeneity of centromere numerical abnormality in multiple primary gastric cancers: Application of fluorescence in situ hybridization with intermittent microwave irradiation on paraffin-embedded tissue. *Jpn J Cancer Res* 2000; **91**: 1134–41.
6 Nakamura R, Song JP, Isogaki J, Kitayama Y, Sugimura H. Multiple (multicentric and multifocal) cancers in the ipsilateral breast with different histologies: Profiles of chromosomal numerical abnormality. *Jpn J Clin Oncol* 2003; **33**: 463–69.
7 Song JP, Kitayama Y, Igarashi H *et al.* Centromere numerical abnormality in the papillary, papillotubular type of early gastric cancer, a further characterization of a subset of gastric cancer. *Int J Oncol* 2002; **21**: 1205–11.
8 Arnould L, Denoux Y, MacGrogan G *et al.* Agreement between chromogenic in situ hybridisation (CISH) and FISH in the determination of HER2 status in breast cancer. *Br J Cancer* 2003; **88**: 1587–91.
9 Todorovic-Rakkovic N, Jovanovic D, Neskovic-Konstaninovic Z, Nikolic-Vukosavljevic D. Comparison between immunohistochemistry and chromogenic in situ hybridization in assessing HER-2 status in breast cancer. *Pathol Int* 2005; **55**: 318–23.
10 Hirohashi S, Kanai Y. Cell adhesion system and human cancer morphogenesis. *Cancer Sci* 2003; **94**: 575–81.

WFL Publisher
Science and Technology
Journal of Food, Agriculture & Environment Vol.3 (2) : 73-76 . 2005
www.world-food.net

# Suppressive effect of epigallocatechin gallate (EGCg) on DNA methylation in mice: Detection by methylation sensitive restriction endonuclease digestion and PCR

**Hidetaka Yamada,[1,2] Haruhiko Sugimura [2] and Toshihiro Tsuneyoshi [1*]**

*[1] Department of Materials Science, Shizuoka Institute of Science and Technology, 2200-2 Toyosawa, Fukuroi, Shizuoka 437-8555, Japan. [2] First Department of Pathology, Hamamatsu University School of Medicine, 1-20-1 Handayama, Hamamatsu, Shizuoka 431-3192, Japan. *e-mail: tuneyosi@ms.sist.ac.jp*

*Received 18 December 2005, accepted 22 March 2005.*

**Abstract**

DNA methylation is a general epigenetic gene alteration that accompanies aging and carcinogenesis. DNA methylation adds a methyl group to the fifth position of cytosine of CpG DNA sequences (also known as CpG island). CpG island methylation in the promoter region of a gene suppresses mRNA expression and subsequent protein expression by inhibiting the transcription factors or recruiting methyl-CpG binding (MBD) proteins and histone deacetylase (HDAC). Recently, Fang et al. showed that the green tea polyphenol constituents, catechins, inhibit DNA methyltransferase (Dnmt1), suppresses DNA methylation, and re-expresses the mRNA and protein of four genes in various human cancer cell lines *in vitro*. Here, we administered epigallocatechin gallate (EGCg)-containing water to mice to observe the effect of EGCg on DNA methylation in the mouse estrogen receptor gene promoter region. We used wild-type and knock-out mice, which had a non-sense mutation in the adenomatous polyposis coli (APC) gene, to compare the effect of EGCg administration on aging and carcinogenesis, respectively. The DNA methylation rate was determined by the digestion of genomic DNA with the methylation-sensitive restriction endonuclease *Ava* I and a polymerase chain reaction (PCR). In the EGCg-administered mice, the methylation rate decreased by 4% in the wild-type mice ($P<0.001$) and 5% in the knock-out mice ($P<0.01$), showing a possible inhibitory effect of EGCg on the epigenetic changes associated with carcinogenesis or aging. To our knowledge, this is the first *in vivo* demonstration of such an effect. The ratio of concentrations producing *in vitro* cytotoxicity and the optimum dose of EGCg is about five times higher than that of zebularine, while the optimum dose of EGCg is 100 times smaller than that of zebularine. EGCg or green tea may be a good candidate material for cancer prevention, anti-aging or cancer treatment without adverse effects.

*Key words:* EGCg, DNA methylation, estrogen receptor, inhibition, restriction endonuclease, PCR.

## Introduction

DNA methylation adds a methyl group to the fifth position of the cytosine of CpG DNA sequences, converting cytosine to 5-methylcytosine. CpG islands are CpG-rich areas, usually located in the vicinity of genes, and are often found near the promoters of widely expressed genes [1]. DNA methylation of CpG islands in the promoter region of housekeeping genes suppresses gene expression by preventing transcription factors from binding to the promoter. Epigenetic gene silencing through this process is thought to be an important step in tumorigenesis and aging [2]. The methylation of several genes increases with age in normal tissues. CpG island methylation of the estrogen receptor (ER) gene occurs in a subpopulation of cells and increases as a direct function of age in normal human colonic mucosa [1]. Age-related methylation increases in a linear manner, although the rate of increase may differ among genes and individuals.

Conventional DNA methylation detection assays involve the digestion of genomic DNA with methylation-sensitive restriction endonuclease (RE) followed by a Southern blot analysis [3]. This technique is straightforward, but requires a large amount of genomic DNA and sometimes involves the use of radioactive materials for DNA labeling. The use of PCR amplification after the digestion of genomic DNA has also been proposed [4], but little attention has been paid to this method. The second type of assays employed the sodium bisulfite treatment of genomic DNA to convert unmethylated cytosines to urasils, while leaving methylated cytosine residues intact before performing PCR [3]. This technique needs only a small amount of genomic DNA; however, the efficiency of bisulfite conversion remains uncertain and controversial [5].

Epigallocatechin gallate (EGCg), a constituent of green tea and a natural polyphenol antioxidant, is known to exhibit anti-mutagenic and anti-tumorigenic effects [6,7]. The anti-aging property of EGCg is being studied by many researchers [8,9]. DNA methylation rate has been shown to increase proportionally with age in many genes, including the ER gene [10]. EGCg may exert its anti-aging property through an inhibitory effect on the DNA methylation of many genes. Recently, EGCg was shown to inhibit DNA methyltransferase, suppress DNA methylation and re-express the mRNA and protein of 4 genes in various human cancer cell lines [11].

Here, we describe, a simple methylation detection method for the ER gene using methylation-sensitive RE and PCR to avoid bisulfite treatment. Using this method, we analyzed the methylation rate of the ER promoter CpG dinucleotide in mice treated with EGCg to determine whether EGCg has a suppressive effect on DNA methylation *in vivo*.

## Materials and Methods

***Model animals:*** To investigate the methylation suppressive effect of EGCg, we administered EGCg to wild-type and APC 1309 knock-out mice [12] to compare the effects of EGCg on aging and carcinogenesis. We used the tail tissue of mice as the source of

DNA extraction, since this method was the easiest way of obtaining body tissue repetitively from the mice. Three male APC 1309 knock-out mice were obtained from the Japanese Foundation for Cancer Research (Cell Biology Department, Cancer Institute, Tokyo, Japan). Male and female APC 1309 knock-out mice were obtained from mice by crossbreeding with wild-type C57BL/6 female mice (Nihon SLC Corp., Shizuoka, Japan). The progeny were genotyped as described elsewhere [13] to ensure their pedigree before breeding if they were heterozygous for the APC 1309 allele or homozygous for the wild-type allele. The wild-type mice used in this experiment consisted of C57BL/6 male and female mice (Nihon SLC Corp., Shizuoka, Japan).

***PCR primers for methylation analysis:*** We focused our methylation analysis experiment on the methylation of ER because the methylation rate of this gene has been shown to increase proportionally with age in humans [10] and with the tumor grade in prostate cancer [14]. Methylation of the CpG island in the ER gene promoter has been observed in breast [15], lung, colorectal [16] and prostate cancer [14] and has been associated with the loss of ER gene expression. Primers ERMS1 (sense) and ERMS2 (antisense) were used to detect the DNA methylation of the ER promoter region (GenBank accession no. M38652) CpG island (Fig. 1) [17]. The primers were designed so that the PCR products (target DNA) included the methylation-sensitive RE, *Ava* I, recognition site (5'-CCCGAG-3') in the CpG island. The primer sequences were 5'-CCTGCCTACTGGCTGCTTCC-3' (ERMS1) and 5'-GACGGAAGGAAGGAATGTGCT-3' (ERMS2). The expected PCR product size was 121bp. Another PCR primer ERMS3 (sense) was designed to generate a control PCR product, which was 20bp longer than the PCR products mentioned above; this product was mixed with genomic DNA and amplified using the same PCR conditions as those for primers ERMS1 and ERMS2, then used as a control band in the gel electrophoresis to normalize the densitometric intensity. In the ERMS3 primer, the *Ava* I recognition site was abolished by inserting a long arbitrary sequence (5'-CGAGAAAAGCTGTTTTTGAT-3', 20-bp) into the original sequence. The final sequence was 5'-CCTGCCTACTGGCTGCTTCCGAGAAAAGCTGTTTTTGATCCGAGAGTCCCTGCCACTCCA-3'. The expected PCR product size was 141bp.

***Preparation of control DNA:*** Genomic DNA extracted from mouse tissue was subjected to PCR using the primers ERMS3 and ERMS2. The PCR products were used as control DNA after purification by phenol/chloroform extraction, ethanol precipitation and a series of dilutions.

***PCR for methylation analysis:*** Genomic DNA extracted from the tails of mice was mixed with the control DNA. The homogeneous mixture was divided equally into two tubes. The digestive reaction was performed at 37°C for 2 hours with the methylation sensitive RE *Ava* I in one tube, and a control mixture without *Ava* I was also incubated in the same manner in another tube. PCR amplification (30 cycles at 94°C for 1 minute, 60°C for 1 minute and 73°C for 1 minute) was performed using the primers ERMS1 and ERMS2. After electrophoresing the PCR products on an agarose gel stained with ethidium bromide, the fluorescent bands of the target DNA and control DNA were photographed. After digitizing the photographic images and subsequent analysis using NIH-image software, the methylation rate was calculated by dividing the band intensity ratio of the target DNA to the control DNA under the conditions of *Ava* I digestion by that without *Ava* I digestion (Fig. 2).

***Calibration curve for the methylation analysis:*** Genomic DNA extracted from mouse tissue was mixed with S-adenosylmethionine and incubated at 37°C for 5 hours with *Sss* I methylase. Genomic DNA treated with *Sss* I methylase was then mixed with intact baby mouse (sacrificed at 1 week of age) genomic DNA at ratios of 8:2, 6:4, 4:6, and 2:8. Equal amounts of control DNA were added to each mixture. The digestive reactions were performed at 37°C for 2 hours with *Ava* I, and mixtures without *Ava* I were also incubated in the same manner to serve as a control. PCR amplification (30 cycles of 94°C for 1 minute, 60°C for 1 minute, and 73°C for 1 minute) was performed using primers ERMS1 and ERMS2. After the agarose gel electrophoresis, a densitometry analysis was performed as stated before. The methylation rate was calculated by dividing the band intensity ratio (target/control DNA) of the digested mixture by that of the non-digested mixture.

***Methylation analysis of EGCg administered mice:*** Four weeks after birth, wild-type and knock-out mice were divided into two groups and given either regular tap water (3 males and 3 females) or 0.05% EGCg-supplemented water (3 males and 3 females). EGCg (95%) was kindly provided by Mitsui Norin (Shizuoka, Japan). A small amount of tail tissue was taken from each mouse at 4, 8 and 12 weeks after birth. These tissues were then used for the DNA methylation detection analysis. The administration experiment had to be terminated at 12 weeks after birth because the knock-out mice began to die from intestinal obstructions after 10 weeks. A Student t-test was used to analyze the effect of EGCg on the DNA methylation rate.

## Results and Discussion

***Calibration of methylation analysis:*** In this study, the methylation rate of the *Ava* I recognition site in the ER promoter region (Fig.1) was determined. As shown in Fig. 2, agarose gel electrophoresis produced control (141bp) and target DNA (121bp) bands. Genomic DNA treated with *Sss* I methylase was mixed with intact mouse (sacrificed at 1 week of age) genomic DNA at ratios of 8:2, 6:4, 4:6, and 2:8. Fig. 3 shows the calibration curve for the methylation rate analysis. The detected methylation rate reproduced the mixing ratio very well ($R^2$=0.9963), although only one experiment was performed for each mixing ratio. Therefore, the calibration curve showed that our methylation-sensitive restriction endonuclease digestion and competitive PCR protocol enabled us to analyze the methylation rate quantitatively.

Many other methods utilize sodium bisulfite to convert unmethylated cytosine to urasil in order to detect the methylated allele rate; however, our method utilized methylation sensitive restriction endonuclease and PCR, similar to the method used by Singer-Sam et al. [4]. Since the converting efficiency of sodium bisulfite treatment remains uncertain [5], we employed the traditional method for detecting methylated nucleotides. Our method, presented here, can detect methylation at only one nucleotide, which is a disadvantage of the present method.

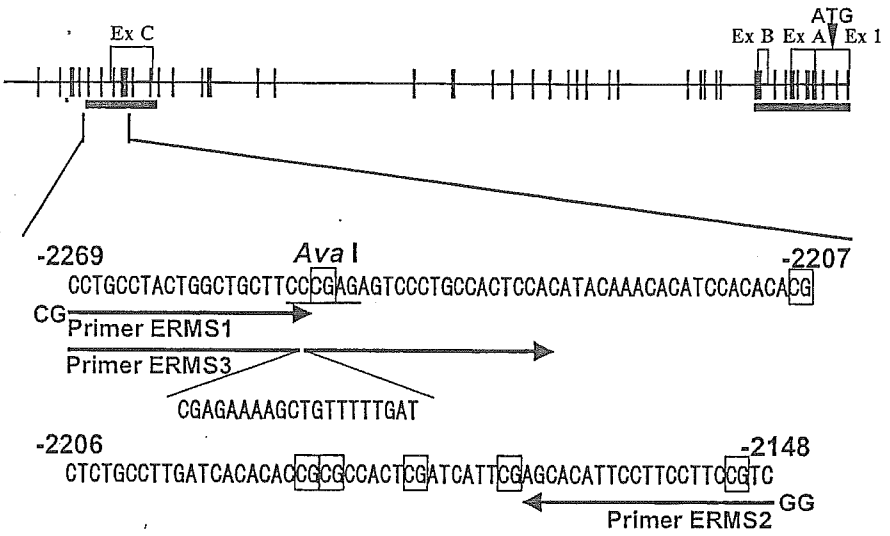


*Figure 1.* PCR primers in the estrogen receptor promoter region for methylation detection. The open squares indicate each exon region, designated by the number or letter after the abbreviation "Ex". The CpG sites are shown by the vertical lines and open squares around the "CG"s. The CpG islands are indicated by the bold underlines near the exons. The recognition site of *Ava* I is indicated by the underline. The numbers indicate the nucleotide positions calculated from the transcription start site. Primers ERMS1 and ERMS2 were used for the methylation analysis. Primers ERMS3 and ERMS2 were used to generate the control DNA. Further details regarding primer ERMS3 are provided in the text.

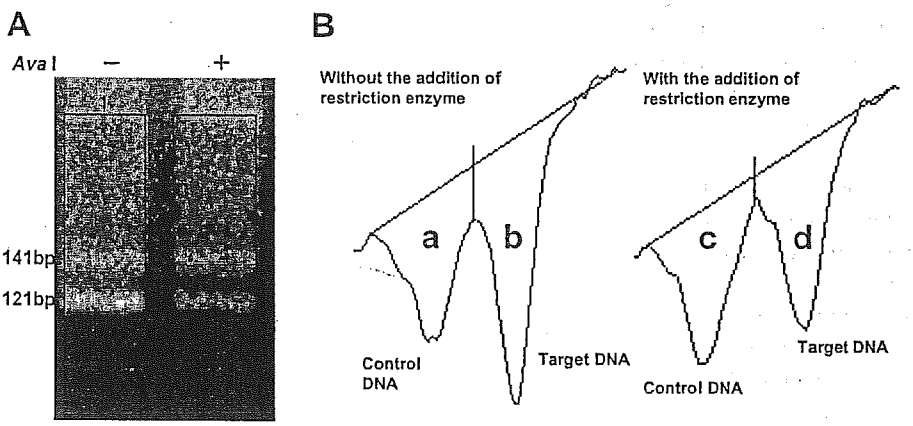


*Figure 2.* Calculation of methylation rate based on gel electrophoresis band intensity. A, Agarose gel electrophoresis showing the *Ava* I digested (+) and non-digested (-) target (121bp) and control (141bp) DNA. B, Densitometry data obtained from the gel bands in A using NIH-image software. a, b, c and d indicate the peak areas of each band. The methylation rate, MR, was calculated using the equation MR = ( a × d ) / ( b × c ).

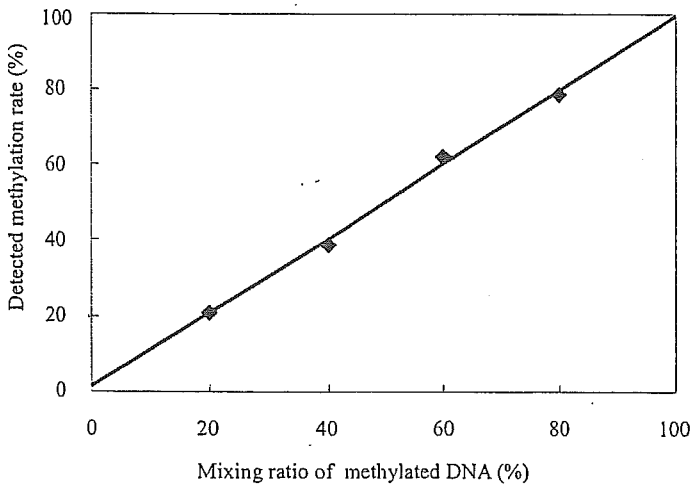


*Figure 3.* Calibration curve for the methylation rate analysis.

***Methylation analysis of EGCg administered mice:*** A comparison of the methylation rates in mice treated with EGCg and in control mice that received tap water is shown in Fig. 4. The methylation rate increased with age in both knock-out and wild-type mice. Thus, the rate of ER methylation seemed to be strongly related to aging. The methylation rate in knock-out mice was about 50% higher than that in wild-type mice, which may be ascribed to the cancer prone-tissues of APC knock-out mice. At 3 weeks of age, when EGCg administration was started, the methylation rates of EGCg-administered and water-administered mice were almost the same. At 12 weeks of age, the methylation rate in the EGCg-administered mice was 5% and 4% lower than that of water-administered knock-out mice ($P<0.01$) and wild-type mice ($P<0.001$), respectively. Therefore, a suppressive effect of EGCg on DNA methylation was observed in both kinds of mice. Tail tissues were repeatedly obtained from the same mice. A wound-healing effect of epicatechin gallate in rats was observed by Kapoor et al. [19]; however, we used mice that had only received tap water for our control.

Silenced tumor suppressor genes are often reactivated by methylation inhibitors, such as 5-azacytidine (5-Aza-CR) and 5-aza-2'-deoxycytidine (5-Aza-CdR) [1]. However, these compounds are chemically unstable or toxic, and none of them can be given safely. Recently, a new demethylating agent, zebularine [1-(beta-D-ribofuranosyl) -1, 2- dihydropyrimidin-2-one], which is a chemically stable cytidine analog, has been synthesized [20]. Zebularine inhibits DNA methylation by forming a covalent complex with DNA methyltransferases.

Zebularine exhibited *in vitro* cytotoxicity in human bladder carcinoma cells at a concentration of 1 mM [18], while EGCg exhibited *in vitro* cytotoxicity in human esophageal squamous cell carcinoma cell lines at a concentration of 50 μM [11], or one-twentieth of 1 mM. However, the optimum doses of zebularine and EGCg for humans or model animals are about 400 mg/kg and 10 mg/kg [6, 7, 20], respectively. Cytotoxicity may be the summation of the regulation of various important genes. Cells and tissues seem to be 20- to 40-fold more sensitive to EGCg than to zebularine, which means that EGCg is a better material for regulating gene expression than zebularine.

The concentration (0.05%) of EGCg that we administered to the mice in this study was around the highest value (1100 μM) that could be expected to not produce toxic or adverse effects *in vivo* and was well-above the $IC_{50}$ value (20 μM) for the inhibition of Dnmt1 [11]. The bioavailability of EGCg in the tail tissue of mice is not known; however, statistically different methylation rates were observed between the water-administered and EGCg-administered mice. Therefore, the EGCg concentration might be around 20-50 μM in the tail tissues, as observed in cell lines by Fang et al. [11]. Compared with 5-Aza-CR, 5-Aza-CdR or zebularine, EGCg is a well-known, commonly consumed and

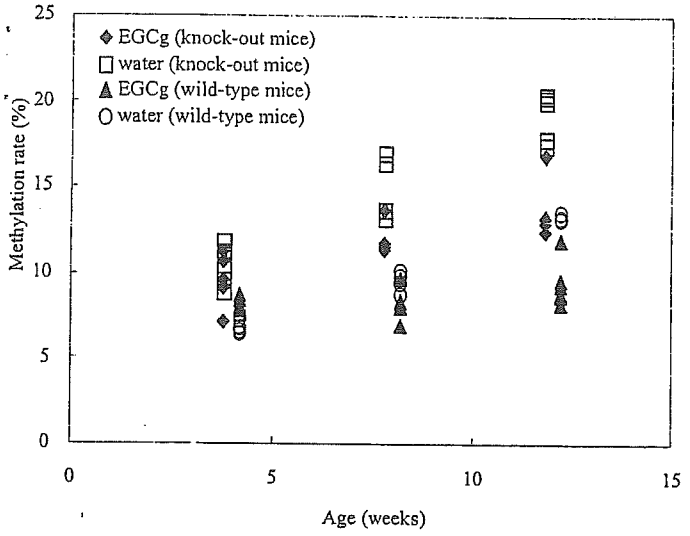


*Figure 4.* Methylation rate of wild-type and knock-out mice. The methylation rates in knock-out and wild-type mice given EGCg or tap water at various age are indicated by the symbols shown in the figure.

well-characterized natural component of green tea that has been consumed from ancient times. Therefore, EGCg is much safer and inexpensive to take or produce as a candidate drug or supplemental materials for cancer treatment, cancer prevention or anti-aging without adverse effects. To our knowledge, this is the first report of the *in vivo* suppressive effect of EGCg on DNA methylation.

## Conclusions

The DNA methylation rate of EGCg-administered knock-out or wild-type mice was statistically lower than that of control mice. Therefore, EGCg appears to have an *in vivo* suppressive effect on DNA methylation caused by carcinogenesis or aging. The ratio of concentrations producing *in vitro* cytotoxicity and the optimum dose of EGCg is about five times higher than that of zebularine, while the optimum dose of EGCg is 100 times smaller than that of zebularine. Thus, EGCg appears to be a better candidate material for cancer treatment, cancer prevention or anti-aging than zebularine. To our knowledge, this is the first report of the *in vivo* suppressive effect of EGCg on DNA methylation.

## Acknowledgement

The authors would like to thank Dr. Satoshi Nakamura, Dr. Yoshiyuki Nakamura and Dr. Kenichi Sunayama for their helpful discussions, Dr. Masato Maekawa, Dr. Yukihiko Hara and Dr. Keiichi Goto for their useful comments on the manuscript. This work was supported by a Grant-in-Aid from the Ministry of Health, Labour, and Welfare (15-5 and 15-22), from the Ministry of Education, Culture, Sports, Science and Technology of Japan for Scientific Research on Priority Area and the 21st century COE program 'Medical Photonics', from the Smoking Research Foundation, from the Foundation for Promotion of Cancer Research, and from the Program for Promotion of Basic Research Activities for Innovating Biosciences (PROBRAIN). H.Y. is a COE research assistant of Hamamatsu University School of Medicine.

## References

[1]Yuasa, Y. 2002. DNA methylation in cancer and aging. Mech. Ageing Dev. **123**: 1649-1654.

[2]Feinberg, A.P. 2001. Cancer epigenetics takes center stage. Proc. Natl. Acad. Sci. USA **98**: 392-394.

[3]Dahl, C. and Guldberg, P. 2003. DNA methylation analysis techniques. Biogerontology **4**: 233-50.

[4]Singer-Sam, J., LeBon, J.M., Tanguay, R.L. and Riggs, A.D. 1990 quantitative HpaII-PCR assay to measure methylation of DNA fr a small number of cells. Nucleic Acids Res. **18**: 687.

[5]Sasaki, M., Anast, J., Bassett, W., Kawakami, T., Sakuragi, and Dahiya, R. 2003. Bisulfite conversion-specific a methylation-specific PCR: a sensitive technique for accur evaluation of CpG methylation. Biochem. Biophys. Res. Comm **309**: 305-309.

[6]Tobi, S.E., Gilbert, M., Paul, N. and McMillan, T.J. 2002. The green polyphenol, epigallocatechin-3-gallate, protects against the oxidati cellular and genotoxic damage of UVA radiation. Int. J. Can **102**:439-444.

[7]Arimoto-Kobayashi, S., Inada, N., Sato, Y., Sugiyama, C., Okamoto, Hayatsu, H. and Negishi, T. 2003. Inhibitory effects (-)-epigallocatechin gallate on the mutation, DNA strand cleavage, a DNA adduct formation by heterocyclic amines. J. Agric. Food Che **51**: 5150-5153.

[8]Lopez-Burillo, S., Tan, D.X., Mayo, J.C., Sainz, R.M., Manchest L.C. and Reiter, R.J. 2003. Melatonin, xanthurenic acid, resveratr EGCG, vitamin C and alpha-lipoic acid differentially reduce oxidati DNA damage induced by Fenton reagents: a study of their individ and synergistic actions. J. Pineal. Res. **34**: 269-277.

[9]Naasani, I., Seimiya, H. and Tsuruo, T. 1998. Telomerase inhibiti telomere shortening, and senescence of cancer cells by tea catechi Biochem. Biophys. Res. Commun. **249**: 391-396.

[10]Ahuja, N., Li, Q., Mohan, A.L., Baylin, S.B. and Issa, J.P. 1998. Agi and DNA methylation in colorectal mucosa and cancer. Cancer R **58**: 5489-5494.

[11]Fang, M.Z., Wang, Y., Ai, N., Hou, Z., Sun, Y., Lu, H., Welsh, W. a Yang, C.S. 2003. Tea polyphenol (-)-epigallocatechin-3-gall inhibits DNA methyltransferase and reactivates methylation-silenc genes in cancer cell lines. Cancer Res. **63**: 7563-7570.

[12]Ito, M., Miura, S. and Noda, T. 1995. Mouse model for famil adenomatous polyposis coli and APC gene. Tanpakushitsu Kakus Koso **40**: 2035-2044.

[13]Quesada, C.F., Kimata, H., Mori, M., Nishimura, M., Tsuneyoshi, and Baba, S. 1998. Piroxicam and acarbose as chemopreventive age for spontaneous intestinal adenomas in APC gene 1309 knockout mi Jpn. J. Cancer Res. **89**: 392-396.

[14]Li, L.C., Chui, R., Nakajima, K., Oh, B.R., Au, H.C. and Dahiya, 2000. Frequent methylation of estrogen receptor in prostate canc correlation with tumor progression. Cancer Res. **60**: 702-706.

[15]Ottaviano, Y.L., Issa, J.P., Parl, F.F., Smith, H.S., Baylin, S.B. a Davidson, N.E. 1994. Methylation of the estrogen receptor gene C island marks loss of estrogen receptor expression in human bre cancer cells. Cancer Res. **54**: 2552-2555.

[16]Issa, J.P., Ottaviano, Y.L., Celano, P., Hamilton, S.R., Davidson, N and Baylin, S.B. 1994. Methylation of the oestrogen receptor C island links ageing and neoplasia in human colon. Nat. Gen **7**: 536-540.

[17]White, R., Lees, J.A., Needham, M., Ham, J. and Parker, M. 19 Structural organization and expression of the mouse estrogen recept Mol. Endocrinol. **1**: 735-744.

[18]Cheng, J.C., Matsen, C.B., Gonzales, F.A., Ye, W., Greer, S., Marqu V.E., Jones, P.A. and Selker, E.U. 2003. Inhibition of DN methylation and reactivation of silenced genes by zebularine. J. N Cancer Inst. **95**: 399-409.

[19]Kapoor, M., Howard, R., Hall, I. and Appleton, I. 2004. Effects epicatechin gallate on wound healing and scar formation in a f thickness incisional wound healing model in rats. Am. J. Path **165**: 299-307.

[20]Driscoll, J.S., Marquez, V.E., Plowman, J., Liu, P.S., Kelley, J.A. a Barchi Jr., J.J. 1991. Antitumor properties of 2(1H)-pyrimidinc riboside (zebularine) and its fluorinated analogues. J. Med. Che **34**: 3280-3284.

# *EPHA2/EFNA1* expression in human gastric cancer

Ritsuko Nakamura,[1] Hideki Kataoka,[2,3] Naomi Sato,[4] Masao Kanamori,[5] Megumi Ihara,[1] Hisaki Igarashi,[1] Sanjar Ravshanov,[1] You-Jie Wang,[6] Zhong-You Li,[7] Takahiro Shimamura,[8] Toshihiko Kobayashi,[8] Hiroyuki Konno,[9] Kazuya Shinmura,[1] Masamitsu Tanaka[10] and Haruhiko Sugimura[1,11]

[1]First Department of Pathology, [2]First Department of Medicine, Hamamatsu University School of Medicine, 1-20-1 Handayama, Hamamatsu 43-3192; [3]Department of Gastroenterology, Hamamatsu Medical Center, 328 Tomitsuka, Hamamatsu 432-8580; [4]Department of Nursing; [5]Department of Lifelong Sport, Biwako Seikei Sport College, 1204 Shigachou, Shigagun, Shiga 520-0503; [6]School of Public Health, Tongi Medical College, #13 Hong Kong Road, Wuhan 430030, China; [7]Department of Cancer Genetics, Roswell Park Cancer Institute, Elm and Carlton Str. Buffalo, NY 14263, USA; [8]First Department of Surgery, and [9]Second Department of Surgery, Hamamatsu University School of Medicine, 1-20-1 Handayama, Hamamatsu 431-3192; and [10]Growth Factor Division, National Cancer Center, 5-1-1 Tsukiji, Cyuo-Ku, Tokyo 104-0045

(Received September 17, 2004/Revised November 15, 2004/Accepted November 16, 2004/Online publication January 19, 2005)

**The erythropoietin-producing hepatocellular (*EPH*)*A2* receptor, tyrosine kinase, is overexpressed and phosphorylated in several types of human tumors and has been associated with malignant transformation. A recent report, however, indicated that stimulation of the *EPHA2* receptor ligand, ephrinA1 (EFNA1), inhibits the growth of *EPHA2*-expressing breast cancer. The authors examined the expression of *EPHA2* and *EFNA1* using semiquantitative reverse transcription-polymerase chain reaction (RT-PCR) in four gastric cancer cell lines and 49 primary gastric cancer samples, as well as in normal gastric tissue. *EPHA2* was more highly expressed in tumor tissue than in normal tissue in 27 cases (55%). *EFNA1* was overexpressed in tumor tissue in 28 cases (57%). No significant correlation was detected between the expression levels and histologic features such as tumor size, age, vessel invasion, or lymph node involvement. However, *EPHA2* overexpression was more prominent in macroscopic type 3 and 4 tumors than in type 1 or 2 advanced gastric cancer. The authors observed *EPHA2* expression in three of the four gastric cancer cell lines (AGS, KATO3, and MKN74) that were examined. In one cell line, TMK1, *EPHA2* expression was barely detectable using northern blotting, RT-PCR, and western blotting. In contrast, *EFNA1* was detected in all cell lines. In the gastric cancer cell lines that endogenously expressed *EPHA2*, stimulation with ephrinA1-Fc led to decreased EPHA2 protein expression and increased EPHA2 phosphorylation. Finally, the growth of *EPHA2*-expressing cells was inhibited by repetitive stimulation with soluble ephrinA1-Fc. Taken together, these findings suggest that *EPHA2* and *EFNA1* expression may influence the behavior of human gastric cancer. (*Cancer Sci* 2005; 96: 42–47)**

The erythropoietin-producing hepatocellular (*EPH*) receptors represent the largest known family of receptor tyrosine kinases and are activated by interaction with the cell-surface ligands, ephrins (*EFN*). There is evidence to suggest that some members of the *EPH* family and their *EFN* ligands are involved in angiogenesis and oncogenesis through cell adhesion, morphogenesis, capillary sprouting, and chemoattraction.[1–5] *EPH* receptors have been classified into two subfamilies, *EPHA* and *EPHB*. *EPHA* receptors bind mainly to glycosylphosphatidylinositol-anchored *EFNA* ligands, and *EPHB* receptors bind to transmembrane *EFNB* ligands. The expression of *EPH* family transcripts has been documented in some melanomas and carcinomas.[6,7] Overexpression of *EPHA2* is believed to be sufficient to confer malignant/tumorigenic potential on non-transformed mammary epithelial cells.[8] Esophageal squamous cell carcinomas that overexpress *EFNA2* have a poorer prognosis than those that do not.[9]

Gastric cancer remains a disease with a very poor prognosis, and the role of kinases in gastric cancer cells has been a focus of research. Ogawa *et al.* identified *EFNA1* and *EPHA2* expression in a very few cases of gastric cancer in 2000, but the role of these molecules has remained unclear,[10] despite an extensive survey of tyrosine kinases in gastric cancer.[11] Therefore, the authors examined the expression of *EPHA2* and *EFNA1* in gastric cancer specimens and gastric cancer cell lines using semiquantitative reverse transcription-polymerase chain reaction (RT-PCR), northern blotting, and western blotting. This is the first documented report of *EFNA1* and *EPHA2* expression in a series of gastric cancer cases. Furthermore, the authors examined the effects of *EFNA1* stimulation on cancer cell lines that endogenously express *EPHA2*.

## Materials and Methods

**Tissues.** For RT-PCR, human gastric cancer specimens and corresponding non-tumor tissues were obtained from 49 surgical resections carried out at Hamamatsu University School of Medicine. The clinicopathologic characteristics of these patients are shown in Table 1, and are classified according to the Japanese classification system (JCS).[12] Histologically, these specimens consisted of 22 cases of well-differentiated adenocarcinoma (tubular and papillary types) and 24 cases of poorly differentiated adenocarcinoma, including the mucinous type, and three other types (two adenosquamous and one neuroendocrine). The samples consisted of six early gastric cancers (the tumor is in the submucosal and mucosal layers in the gastric wall) and 43 advanced gastric cancers (the tumor invades through the proper muscle layer of the gastric wall). According to the pathologic TNM classification, there were 18 cases at stages I and II, and 31 cases at stages III and IV. All samples were immediately frozen in liquid nitrogen and stored at −80°C until RNA preparation was carried out. The study design was approved by the Institutional Review Board of Hamamatsu University School of Medicine (no. 12–11).

**Cell cultures.** Gastric cancer cell lines (KATO3, MKN74, and TMK1) were cultured in RPMI 1640 (Nissui, Tokyo, Japan) supplemented with 10% fetal bovine serum (FBS; Gibco Invitrogen, Carlsbad, CA, USA). The AGS cells were cultured in Ham's F12K medium (ICN Biomedicals, Bryan, OH, USA) supplemented with 10% FBS. The 293T human embryonic kidney cells were cultured in Dulbecco's modified eagle medium (Nissui) supplemented with 10% FBS.

**RNA extraction and reverse transcription.** Total cellular RNA was extracted from human tissues using the RNA extraction reagent, ISOGEN, (Nippon Gene, Tokyo, Japan) according to the manufacturer's protocol. Single-stranded cDNA was prepared from total RNA and 1 μg of oligo dT primer (Life Technologies, Rockville, MD, USA) in a total volume of 20 μL containing Moloney murine leukemia virus reverse transcriptase (Life Technologies) and RNase inhibitor (Toyobo, Tokyo, Japan).

[11]To whom correspondence and reprint requests should be addressed. E-mail: hsugimur@hama-med.ac.jp



 doi: 10.1111/j.1349-7006.2005.00007.x

Table 1. The correlation between EPHA1 and EPHA2 expression and the clinicopathologic parameters

| | No. | EPHA2 | | EFNA1 | |
|---|---|---|---|---|---|
| | | Average of log T/N | *P*-value | Average of log T/N | *P*-value |
| Male | 38 | 0.25406 | 0.162§§ | 0.135515 | 0.913§§ |
| Female | 11 | −0.05075 | | 0.152799 | |
| Histologic type† | | | | | |
| tub1, 2 and pap | 22 | 0.1897 | 0.995¶¶ | 0.218730 | 0.463¶¶ |
| por 1, 2 and muc | 24 | 0.186329 | | 0.093821 | |
| Others | 3 | 0.150229 | | −0.778000 | |
| Macroscopic type‡ | | | | | |
| 1 and 2 | 15 | 0.014809 | 0.029§§ | 0.124345 | 0.689§§ |
| 3 and 4 | 26 | 0.380546 | | 0.058599 | |
| Depth of tumor invasion | | | | | |
| T1 (m and sm)§ | 6 | −0.30717 | 0.041§§ | 0.241157 | 0.738§§ |
| T2, 3 and 4 (mp, ss, se and si)¶ | 43 | 0.254396 | | 0.125196 | |
| Stage | | | | | |
| I (IA and IB) | 11 | 0.192919 | 0.298¶¶ | 0.179152 | 0.630¶¶ |
| II | 7 | 0.692538 | | 0.196717 | |
| III (IIIA and III B) | 22 | 0.09198 | | 0.176363 | |
| IV | 9 | 0.011395 | | −0.044150 | |
| Lymph node metastasis | | | | | |
| (−)†† | 15 | 0.302749 | 0.483§§ | 0.182655 | 0.665§§† |
| (+)‡‡ | 34 | 0.133964 | | 0.120310 | |
| Lymphatic invasion | | | | | |
| ly0 and 1 | 31 | 0.271833 | 0.142§§ | 0.193581 | 0.514§§ |
| ly2 and 3 | 18 | 0.035413 | | 0.108180 | |
| Venous invasion | | | | | |
| v0 | 17 | 0.134045 | 0.912††† | 0.200282 | 0.866††† |
| v1 | 16 | 0.279166 | | 0.120467 | |
| v2 | 10 | 0.12316 | | 0.140152 | |
| v3 | 6 | 0.186497 | | 0.016096 | |

†tub1, tubular adenocarcinoma, well-differentiated type; tub2, tubular adenocarcinoma, moderately differentiated type; pap, papillary adenocarcinoma; por1, poorly differentiated adenocarcinoma, solid type; por2, poorly differentiated adenocarcinoma, non-solid type; muc, mucinous adenocarcinoma; others, adenosquamous carcinoma and neuroendocrine carcinoma. ‡Except type 0, superficial, flat tumors and type 5, non-classifiable carcinomas. §This category is called 'early cancer'. ¶This category is called 'advanced cancer'. ††'N0' using the Japanese classification system (JCS).[12] ‡‡'N1, N2 and N3' using the JCS.[12] §§Student's *t*-test. ¶¶Kruskal–Wallis test. †††ANOVA.

**Semiquantitative RT-PCR analysis.** The semiquantitative RT-PCR method used in this study was modified from a previously described method.[13] Briefly, cDNA was diluted in water, and mixed in a final volume of 20 μL with 0.625 μmol/L of primer pairs, 1 U of Taq DNA polymerase (Roche, Basel, Switzerland), and 1 μCi of [γ-$^{32}$P] dCTP (Amersham Biosciences, Piscataway, NJ, USA). Amplification was carried out in a DNA thermal cycler (PC-700; ASTEC, Fukuoka, Japan). For the human β-actin (*ACTB*) control, 30 cycles were carried out, consisting of denaturation for 45 s at 94°C, followed by primer annealing for 1 min at 59°C, polymerization for 1 min at 72°C, and final extension for 10 min at 72°C. For *EPHA2* and *EFNA1*, 35 cycles were carried out, consisting of denaturation for 45 s at 94°C, primer annealing for 1 min at 59°C, polymerization for 1 min at 72°C, and final extension for 10 min at 72°C. Under these conditions, PCR was carried out during the exponential phase of amplification for *ACTB*, *EPHA2*, and *EFNA1*. A negative control was added to exclude the possibility of DNA contamination in each reaction. The integrity of the RNA obtained from the clinical samples was confirmed by determining the presence of *ACTB* mRNA in the same samples, and the 28S and 18S peaks using Agilent 2100 Bioanalyzer (Agilent Technology, Waldbrown, Germany). The sizes of *ACTB*, *EPHA2*, and *EFNA1* were 121 base pairs (bp), 260 bp, and 230 bp, respectively. The primer sequences were as follows: (a) *EPHA2*, 5′-GCAACATCCTCGTCAACAGC-3′ (sense primer) and 5′-TGGCTTTCATCACCTCGTGG-3′ (antisense primer); (b) *EFNA1*, 5′-AACAA-GCTGTGCAGGCATGG-3′ (sense primer) and 5′-CTCCACAGATGAGGTCTTGC-3′ (antisense primer); (c) *ACTB*, 5′-GCTACGTCGCCCTGGACTTC-3′ (sense primer) and 5′-AGCGGAACCGCTCATTGCCA-3′ (antisense primer). The PCR products were separated using electrophoresis on 6% polyacrylamide gels, which were then dried and autoradiography and image analysis was carried out using MacBAS (Fuji Film, Tokyo, Japan). Representative cases showing expression of *EFNA1*, *EPHA2*, and *ACTB* in gastric cancer and the corresponding non-tumor specimens are shown in Figure 1.

**Statistical analysis.** The autoradiographic densities were transformed into common logarithms. For statistical comparisons of the log-transformed data between two or more groups, an ANOVA was used when the variances of the groups were equal, and the Kruskal–Wallis test was used when the variances were not equal. When simply comparing two groups, Student's *t*-test was used. Levene's test was used to assess the equality of the variance for all group comparisons. Wilcoxon's signed-rank test, based on the rank of the differences between each pair of tissues in the observation, was also used. All statistical analyses were carried out using the SPSS software program version 11.5J (SPSS Japan, Tokyo, Japan). The statistical tests were two-sided, and the results were considered to be significant when the *P*-value was $<0.05$.

**Northern blotting.** Twenty micrograms of total RNA for each of *ACTB*, *EPHA2*, and *EFNA1* was separated on 1.0% denatured agarose gels, and blotted on NitroPlus (Micron Separations, Westboro, MA, USA) for 16 h. The plasmids, pAlterMAX, containing *EFNA1* and *EPHA2* cDNA (Gene Bank accession

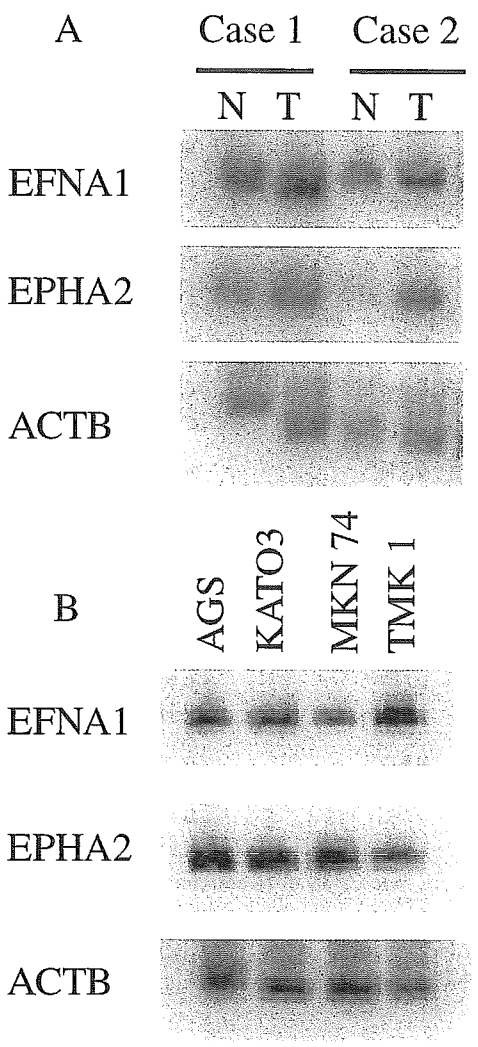


**Fig. 1.** Semi-quantitative reverse transcription-polymerase chain reaction data of two cases of primary gastric cancer and corresponding non-tumor tissue, and gastric cancer cell lines. (A) Both ephrinA1 (EFNA1) and EPHA2 were overexpressed in these tumors (cases 1 and 2). ACTB is shown as an internal control. (B) EFNA1 was expressed in all gastric cell lines, particularly in TMK1. EPHA2 was detected in these four cell lines, but expression was weak in TMK1 compared with the other lines. N, non-tumorous gastric tissue; T gastric cancer tissue.

numbers NM_004428 and NM_004431, respectively), have been described previously.[14] Specific probes were constructed from these plasmids using digestion, with the following appropriate restriction enzymes, *Eco*RI and *Bam*HI (for *EFNA1*) or *Not*I and *Bam*HI (for *EPHA2*). 18S RNA was used as a control. The probes were labeled with $^{32}$P-dCTP using a random primed DNA labeling kit (Takara, Otsu, Japan). Hybridization was carried out at 42°C for 10 h. The hybridized membranes were washed three times at 42°C for 10 min and three times at 65°C for 30 min in 0.1% sodium dodecylsulfate (SDS) and 0.1× standard saline citrate. For normalization of signal intensity, the membranes were stripped and then rehybridized with an 18S probe. The autoradiographic densities were measured using a bio-imaging analyzer (BAS-1000; Fuji Film).

**Protein extraction from tissue.** Proteins were extracted from gastric cancer tissue and from non-tumor gastric tissue, dissected, and identified microscopically. They were powdered and homogenized in TXB (10 m*M* Tris [pH 7.6], 150 m*M* NaCl, 5 m*M* ethylenediamine tetra-acetic acid [EDTA], 10% glycerol, 1 m*M* $Na_3VO_4$, 1% TritonX-100, aprotinin [10 μg/mL], leupeptin [10 μg/mL], and phenyl-methyl-sulfonyl-fluoride [PMSF; 20 μg/mL]). After keeping on ice for 30 min, the proteins were centrifuged twice at 18 000 × *g* for 30 min. These lysates were then used for western blotting.

**EPH receptor stimulation, immunoprecipitation, and western blots.** A soluble form of ephrinA1-Fc, which is a mouse ephrinA1-human IgG1 Fc chimeric protein, was purchased from R&D Systems (Minneapolis, MN, USA). Human IgG1 Fc protein was used as a control (R&D Systems). The proteins were clustered using antihuman IgG, $Fc_\gamma$ (Jackson Immuno Research Laboratories, West Grove, PA, USA) in RPMI with 0.5% FBS. The cells were incubated for 1 day, and then fed with a medium containing the clustered chimeric protein at 37°C. At the indicated times after stimulation, cells were harvested in lysis buffer (50 m*M* HEPES, 150 m*M* NaCl, 10% glycerol, 1% Triton X-100, 1.5 m*M* $MgCl_2$, 1 m*M* ethyleneglycol-bis[β-aminoethyl ether]-*N*,*N*,*N*′,*N*′-tetra-acetic acid, 10 m*M* $Na_4P_2O_7$, 100 m*M* NaF, 1 m*M* $Na_3VO_4$) in the presence of protease inhibitors (aprotinin [10 μg/mL], leupeptin [10 μg/mL], and PMSF [20 μg/mL]). To pull down phosphorylated EPHA2, the cell lysates were incubated with anti-EPHA2 antibody (clone D7; Upstate Biotechnology, Lake Placid, NY, USA) followed by precleaning and immunoprecipitation with protein G sepharose (Amersham Biosciences). Immunoprecipitated lysates were then separated using sodium dodecyl sulfate–polyacrylamide gel electrophoresis (SDS–PAGE), transferred to nitrocellulose membranes (Amersham Biosciences), and immunoblotted with antiphosphotyrosine antibody (Upstate Biotechnology). The total lysate was also loaded in parallel for comparison.

**Immunohistochemistry.** The formalin-fixed paraffin-embedded gastric cancer tissue next to the portions taken for RNA and protein analysis was immunostained with anti-EPHA2 (C-20, dilution 1:100; Santa Cruz Biotechnology, Santa Cruz, CA, USA) according to the manufacturer's instructions. We gathered nine cases of gastric adenoma and immunostained these in the same manner.

Antibody specificity was demonstrated using an immunoabsorption test with 6 μg/mL of EPHA2(C-20) blocking peptide (Santa Cruz Biotechnology). All the immunostains in this study were accompanied by this absorption test. The specificity of this antibody has also been tested by carrying out western blotting with this antibody to the lysate of 293T cells that were transfected with a plasmid that encoded EPHA2.

**Cell growth assay.** A quantity of $1 \times 10^5$ cells of MKN74 and TMK1 was seeded into each well of a six-well tissue culture dish (Greiner Bio-one, Kremsmüster, Austria). The cells were replenished with a medium that contained clustered ephrinA1-Fc (4 μg/mL) or clustered Fc every 24 h. After 3 days of incubation at 37°C, cells were harvested in trypsin-EDTA solution (0.05% Trypsin, 0.53 m*M* EDTA-4 Na; Invitrogen, Carlsbad, CA, USA) and the number of cells was counted using a hemacytometer. The experiment was repeated at least three times. Statistical analysis was carried out using Student's *t*-test (Microsoft Excel, Seattle, WA, USA), with $P < 0.05$ defined as significant.

## Results

**Expression of EPHA2 and EFNA1 in gastric cancer tisseus, paired non-tumor tissues, and gastric cancer cell lines.** The authors examined the expression of *EPHA2* and *EFNA1* RNA in cancerous and non-cancerous gastric tissue using semiquantitative RT-PCR analysis (Fig. 1A). *EPHA2* was more highly expressed in tumor tissues than in normal tissues in 27 of 49 cases (55%). *EFNA1* was also overexpressed in substantial subsets of tumor tissues relative to the normal counterparts, specifically in 28 of 49 cases (57%). When classified using histology, *EPHA2* overexpression


 doi: 10.1111/j.1349-7006.2005.00007.x

was more frequently detected in poorly differentiated adenocarcinoma (14/24 [58%]) than in well-differentiated adenocarcinoma (11/22 [50%]). Overexpression of *EFNA1* was more frequently detected in well-differentiated (15/22 [68%]) than in poorly differentiated adenocarcinoma (14/24 [58%]). However, these trends were not statistically significant. Generally, simultaneous expression of *EPHA2* and *EFNA1* in individual cases was not noted. Rather, the expression pattern was somewhat reciprocal.

When the authors classified the expression of both genes based on the depth of tumor invasion, *EPHA2* overexpression was more prominent in tumors that invaded deeper than the proper muscle layer of the gastric wall than in those that were within the mucosal and submucosal layers (depth mp, ss, se, and si *vs* depth m and sm, $P = 0.041$; lower-case abbreviations used as given in the JCS).[12] Furthermore, when the advanced cases ($n = 43$) were categorized into four macroscopic types according to the JCS, more frequent overexpression of EPHA2 was noted in type 3 and 4 tumors. That is, overexpression was more common in tumors that were macroscopically infiltrating with undefined margins or infiltrating diffusely, than in type 1 and 2 tumors, which are polypoid or ulcerated tumors with sharply demarcated margins ($P = 0.029$).

As for lymphatic invasion, it is difficult to estimate when tumor cells proliferate and are accompanied by severe stromal fibrosis. Therefore, the authors defined lymphatic invasion as 'mild' (corresponding to ly0 and ly1 in the JCS) or 'severe' (corresponding to ly2 and ly3 in the JCS). In cases with mild lymph vessel invasion, *EPHA2* was more frequently overexpressed than in cases with severe invasion, although this difference was not statistically significant ($P = 0.14$). No other significant correlations were detected when compared with age, lymph node involvement, or vessel invasion. A summary of the correlation between *EPHA2* and *EFNA1* expression and clinicopathologic characteristics is shown in Table 1.

The authors monitored EPHA2 protein expression in the gastric cancer tissues using immunohistochemistry and western blotting (Fig. 2). EPHA2 overexpression in cancer tissue compared with non-tumor tissue was confirmed in those cases in which EPHA2 overexpression was demonstrated using RT-PCR (Fig. 1A, case 2). In this case, EPHA2 was detected in a cancerous portion (Fig. 2A). The EPHA2 staining in the cancerous portion disappeared when absorption with EPHA2-blocking peptide, supplied by Santa Cruz, was carried out (Fig. 2B). Western blotting using this antibody to transfected cells further verified the specificity of the antibody (Fig. 2C).

The authors noted that RT-PCR data in some cases indicated considerable EPHA2 expression in non-tumorous gastric tissue. Immunohistochemical analysis of such cases demonstrated that EPHA2 immunoreactivity was detected not only in cancerous portions, but also in non-tumorous mucosa, mostly in that with intestinal metaplasia (Fig. 2D). Additionally, of the nine cases of adenomas that were investigated, three cases showed immunoreactivity to EPHA2, while the others did not show any (Fig. 2E,F).

In the cases that had EPHA2 overexpression in cancerous tissue, the authors could confirm EPHA2 overexpression using western blotting (Fig. 2G). Together, these data indicate that a substantial portion of gastric cancer, particularly infiltrative advanced cancer, is characterized by EPHA2 overexpression.

**EPHA2 expression and phosphorylation by ephrinA1-Fc stimulation in gastric cancer cell lines.** The *EPHA2* and *EFNA1* expression profiles in four gastric cancer cell lines were examined using RT-PCR. *EPHA2* was clearly detected in three gastric cancer cell lines (AGS, KATO3 and MKN74), but the band in TMK1 was fainter than that in the other three cell lines (Fig. 1B). In contrast, *EFNA1* seemed to be more abundantly expressed in TMK1 than in the other three cell lines (Fig. 1B). These data were also confirmed using northern blotting (Fig. 3). The

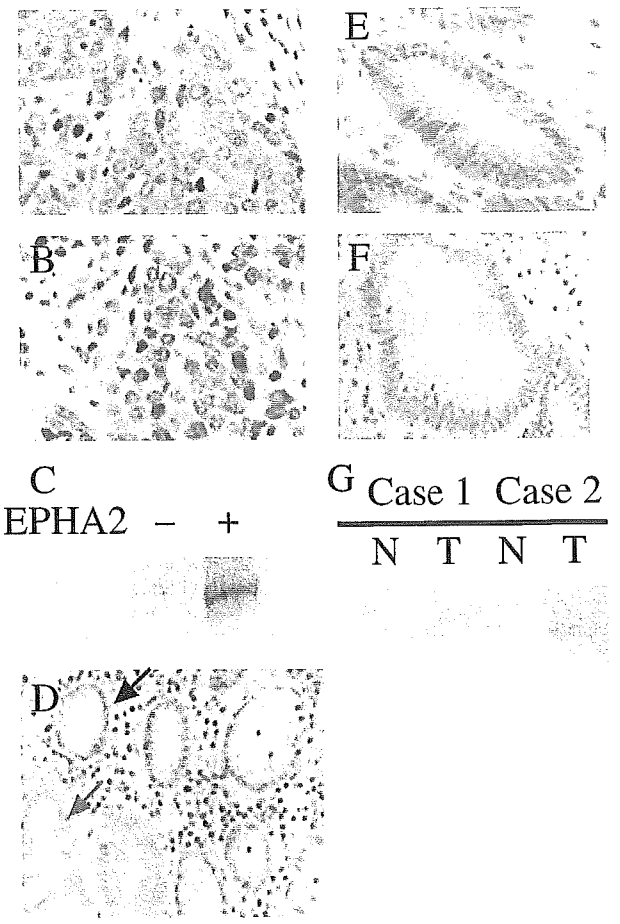


**Fig. 2.** Immunohistochemistry of EPHA2 in primary gastric cancer tissue. (A) EPHA2 was detected in cytoplasm and cell membrane of tumor cells. ×400. (B) The adjacent section after absorption with EPHA2 blocking peptide. ×400. (C) Western blotting using anti-EPHA2 antibody to cell lysates of 293T transfected with a mock (–) and an EPHA2 encoding plasmid (+). (D) Normal (black arrow) and intestinal metaplasia (red arrow) portion. ×400. (E,F) Gastric adenomas with (E) and without (F) EPHA2 immunoreactivity. (G) Western blotting of the primary tissues to anti-EPHA2 antibody. Case 1 and 2 are the same cases 1 and 2 shown in Fig. 1A. The lysates were from N (non-tumorous gastric tissue) and T (gastric cancer tissue).

authors believe the prevalence of *EPHA2* expression in gastric cancer cell lines (three of four) is consistent with that in primary gastric tumor tissue described above. Using MKN74, in which *EPHA2* expression is prominent, the effects of the soluble ligand, EFNA1, on the EPHA2 expression level and on phosphorylation were investigated. Interestingly, and as expected from the authors' previous data,[14] when MKN74 cells were stimulated by clustered ephrinA1-Fc chimeric protein, the EPHA2 phosphorylation increased and the EPHA2 protein degraded (Fig. 4). Both phenomena were dose- and time-dependent. The same results were also obtained for other *EPHA2*-expressing gastric cancer cell lines (AGS and KATO3; Fig. 4C). TMK1, in which *EPHA2* was faintly expressed, showed no change in expression and phosphorylation level as a result of ephrinA1-Fc stimulation.

**EFNA1–EPHA2 signals inhibit cell growth.** The authors further tested the effect of the ligand on anchorage-dependent growth of *EPHA2*-expressing gastric cancer cell lines. As shown in Figure 5, the growth of MKN74 was retarded by stimulation of soluble ephrinA1-Fc every 3 days, compared with cells treated with the control Fc protein ($P < 0.05$, using Student's *t*-test; Fig. 5). In contrast, in TMK1, which very weakly expresses EPHA2, cell growth was not changed by ephrinA1-Fc ($P = 0.53$; Fig. 5).

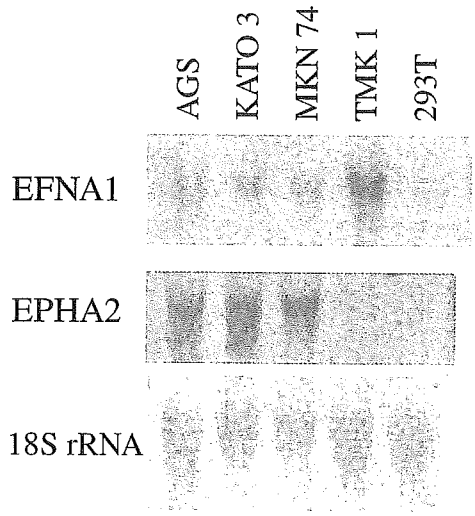


**Fig. 3.** EphrinA1 (EFNA1) and EPHA2 expression by northern blotting. (A) EFNA1 is expressed in all gastric cancer cell lines, particularly TMK1. (B) EPHA2 is clearly detected in AGS, KATO3, and MKN74, but very weakly in TMK1. These data were quantitatively consistent with those obtained using semiquantitative reverse transcription-polymerase chain reaction, shown in Figure 1. 293T is shown as a negative control.

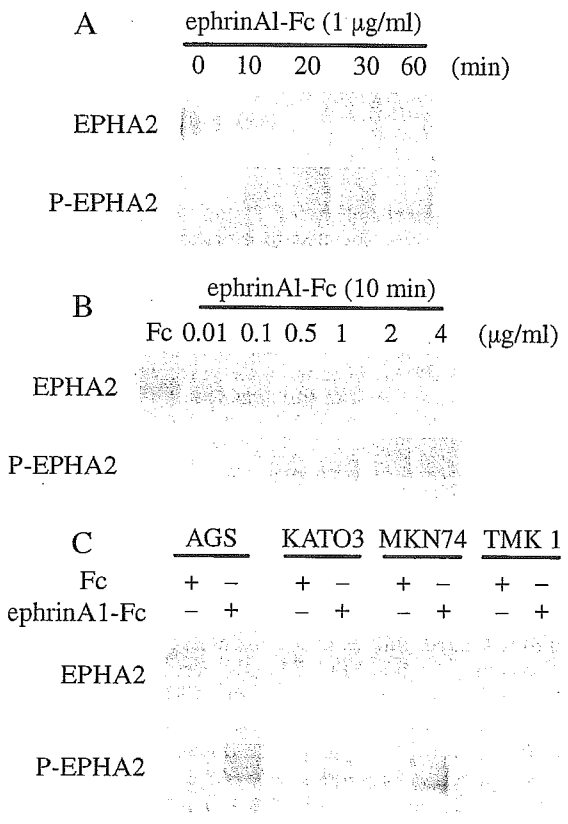


**Fig. 4.** Phosphorylation and degradation of EPHA2 stimulated by ephrinA1-Fc in MKN74 cells and other gastric cell lines. (A,B) MKN74 cells were stimulated by ephrinA1-Fc for the indicated periods (A) and at the noted concentrations (B). Total cell lysates were separated using sodium dodecyl sulfate–polyacrylamide gel electrophoresis (SDS–PAGE) and immunoblotted with anti-EPHA2 antibody (upper panels). The cell lysates were immunoblotted with antiphosphotyrosine antibody after immunoprecipitation with anti EPHA2 and separated using SDS–PAGE (lower panels). (C) EPHA2 expression after EFNA1 stimulation in the other gastric cancer cell lines. AGS and KATO3 also showed an increase in EPHA2 phosphorylation and degradation of EPHA2 by ephrinA1-Fc.

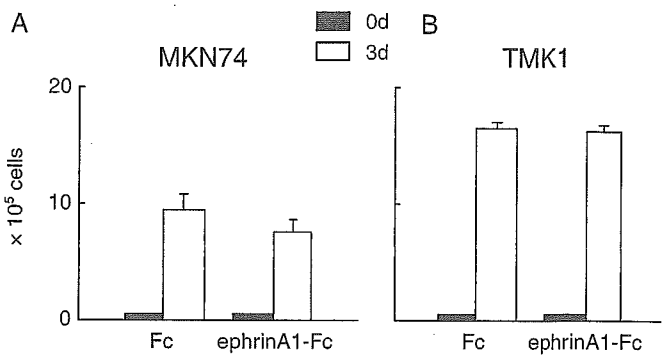


**Fig. 5.** EphrinA1-Fc inhibited growth of cells expressing EPHA2, but not cells that did not express EPHA2. (A) $1 \times 10^5$ of MKN74 or (B) TMK1 were seeded on a six-well dish and, after 24 h, fed with cell medium containing ephrinA1-Fc. The medium was changed every 24 h for 3 days, and the cell numbers were counted using a hemacytometer daily. EFNA1 stimulation inhibited MKN74 cell growth. The bars show means ± SE of cell numbers (three or more experiments).

## Discussion

Receptor tyrosine kinases and their ligands play a critical role in regulation of cellular survival, proliferation, and differentiation.[15–17] *EPH* and *EFN* overexpression have been documented in many types of tumors, including gastrointestinal carcinoma. The authors have previously reported that *EPHB2* and *EFNB1* are overexpressed in gastric cancer.[18,19] With regard to *EPHA2*, a well-documented epithelial type EPH kinase, several studies have shown *EPHA2* overexpression in breast cancer,[8] advanced melanoma,[20] non-small-cell lung carcinoma,[20,21] prostate cancer,[23–25] renal cell carcinoma,[26] esophageal cancer,[9] and colorectal cancer.[10,13,27] Furthermore, as the authors have previously reported, *EPHA2* overexpression sometimes confers an angiogenic phenotype to colon tumors.[13]

The expression of *EFNA1* and *EPHA2* in 49 primary gastric cancer tissues and corresponding non-cancerous mucosa was examined in the present report. The authors found preferential *EPHA2* overexpression in advanced gastric cancer and, interestingly, in tumors with diffuse infiltrating margins with the surrounding tissue (macroscopic types 3 and 4).

Previous *in vitro* studies of breast cancer, pancreatic cancer, and malignant melanoma have shown that overexpression of *EPHA2* promotes malignant features of tumor cells, such as aggressiveness of cell growth, cellular invasiveness[28] and migration. EFNA1 or EPHA2 antibodies have been shown to negatively regulate EPHA2 expression and migration in human and rodent systems.[8,29–31] In light of these previous reports, the preferential overexpression in infiltrative and advanced gastric cancers reported here verifies the role of these molecules in human gastric carcinogenesis, in a physiological context. Overexpression of *EPHA2* gives gastric cancer more infiltrative characteristics.

There were some cases in which EPHA2 was detected in non-tumor tissue. As far as additional immunohistochemical analysis was extended to the premalignant gastric mucosae, EPHA2 was detectable in some, but not in all of these background mucosae (normal and intestinal metaplasia), as shown in Fig. 2D. It appears that the portions that were randomly selected and analyzed using RT-PCR, in some cases showed EPHA2 expression in the non-tumorous tissue. The authors also investigated gastric adenomas and found modest immunoreactivity in some (Fig. 2E,F). Generally, the immunoreactivity in the non-cancerous epithelial portion was less intense and more localized. However, there are a few reports of *EFNA1* expression profiles in human tumors. The authors also investigated the expression of *EFNA1*


 doi: 10.1111/j.1349-7006.2005.00007.x

in gastric cancer, and some samples were found to overexpress *EFNA1*. However, the profile is not like that of *EPHA2*. For example, although not statistically significant, the *EFNA1* expression level seems to be lower in well-differentiated than in poorly differentiated adenocarcinoma, which is contrary to the situation for *EPHA2*. Moreover, in terms of the macroscopic type and the depth of tumor invasion in the gastric wall, the *EFNA1* expression profile was the reverse of that of *EPHA2*. The authors inferred that the following *in vitro* study would give some insight to explain this observation. Cell lines with high levels of EPHA2 (AGS, KATO3, and MKN74) exhibit lower levels of EFNA1, whereas those expressing high levels of EFNA1 (TMK1) exhibit lower levels of EPHA2. EPHA1 stimulation leads to EPHA2 degradation.

Further, the authors showed that EFNA1–EPHA2 participated in anchorage-dependent growth of gastric cancer cell lines. This seems to be related to the *EPHA2* status, because TMK1, a cell line that expresses a lower level of *EPHA2*, did not respond to EFNA1 stimulation.

Concerning the mechanism of *EPHA2* degradation involving ligand-mediated autophosphorylation and degradation, the authors have already reported a contribution from c-CBL, an adapter protein.[14,32] In the present study, when MKN74 was stimulated by ephrinA1-Fc, the binding of EPHA2 and c-CBL by co-immunoprecipitation was detected (data not shown). Thus, EFNA1-induced downregulation of EPHA2, described here in gastric cancer, also probably occurs through CBL–EPHA2 interaction.

In the present report the authors showed the *EPHA2* and *EFNA1* expression profiles in gastric cancer and gastric cancer cell lines. *EPHA2* expression, phosphorylation, and growth were regulated by EPHA1 in gastric cancer cell lines. Considering that several investigators are expecting EPHA2/EFNA1 to be a molecular target for therapy against pancreatic cancer,[28,29] it is plausible that this may also be the case with advanced gastric cancer.

## Acknowledgments

This research was supported by Grants-in-Aids for Scientific Research on Priority Areas and a COE grant (Hamamatsu University School of Medicine, Medical Photonics) from the Ministry of Education, Culture, Sports, Science, and Technology of Japan, and grants from the Ministry of Health, Labour, and Welfare of Japan, the Smoking Research Foundation, and the Foundation for Promotion of Cancer Research.

## References

1 Bohme B, VandenBos T, Cerretti DP, Park LS, Holtrich U, Rubsamen-Waigmann H, Strebhardt K. Cell-cell adhesion mediated by binding of membrane-anchored ligand LERK- 2 to the EPH-related receptor human embryonal kinase 2 promotes tyrosine kinase activity. *J Biol Chem* 1996; **271**: 24747–52.
2 Mellitzer G, Xu Q, Wilkinson DG. Eph receptors and ephrins restrict cell intermingling and communication. *Nature* 1999; **400**: 77–81.
3 George SE, Simokat K, Hardin J, Chisholm AD. The VAB-1 Eph receptor tyrosine kinase functions in neural and epithelial morphogenesis in C. elegans. *Cell* 1998; **92**: 633–43.
4 Adams RH, Wilkinson GA, Weiss C, Diella F, Gale NW, Deutsch U, Risau W, Klein R. Roles of ephrinB ligands and EphB receptors in cardiovascular development: demarcation of arterial/venous domains, vascular morphogenesis, and sprouting angiogenesis. *Genes Dev* 1999; **13**: 295–306.
5 Pandey A, Shao H, Marks RM, Polverini PJ, Dixit VM. Role of B61, the ligand for the Eck receptor tyrosine kinase, in TNF- alpha-induced angiogenesis. *Science* 1995; **268**: 567–9.
6 Hafner C, Schmitz G, Meyer S, Bataille F, Hau P, Langmann T, Dietmaier W, Landthaler M, Vogt T. Differential gene expression of Eph receptors and ephrins in benign human tissues and cancers. *Clin Chem* 2004; **50**: 490–9.
7 Easty DJ, Herlyn M, Bennett DC. Abnormal protein tyrosine kinase gene expression during melanoma progression and metastasis. *Int J Cancer* 1995; **60**: 129–36.
8 Zelinski DP, Zantek ND, Stewart JC, Irizarry AR, Kinch MS. EphA2 overexpression causes tumorigenesis of mammary epithelial cells. *Cancer Res* 2001; **61**: 2301–6.
9 Miyazaki T, Kato H, Fukuchi M, Nakajima M, Kuwano H. EphA2 overexpression correlates with poor prognosis in esophageal squamous cell carcinoma. *Int J Cancer* 2003; **103**: 657–63.
10 Ogawa K, Pasqualini R, Lindberg RA, Kain R, Freeman AL, Pasquale EB. The ephrin-A1 ligand and its receptor, EphA2, are expressed during tumor neovascularization. *Oncogene* 2000; **19**: 6043–52.
11 Kao HW, Chen HC, Wu CW, Lin WC. Tyrosine-kinase expression profiles in human gastric cancer cell lines and their modulations with retinoic acids. *Br J Cancer* 2003; **88**: 1058–64.
12 Japanese Gastric Cancer Association. Japanese classification of gastric carcinoma – 2nd English edition. *Gastric Cancer* 1998; **1**: 10–24. Available from URL: http://www.jgca.jp/PDFfiles/JCGC-2E.PDF
13 Kataoka H, Igarashi H, Kanamori M, Ihara M, Wang JD, Wang YJ, Li ZY, Shimamura T, Kobayashi T, Maruyama K, Nakamura T, Arai H, Kajimura M, Hanai H, Tanaka M, Sugimura H. Correlation of EPHA2 overexpression with high microvessel count in human primary colorectal cancer. *Cancer Sci* 2004; **95**: 136–41.
14 Wang Y, Ota S, Kataoka H, Wang Y, Ota S, Kataoka H, Kanamori M, Li Z, Band H, Tanaka M, Sugimura H. Negative regulation of EphA2 receptor by Cbl. *Biochem Biophys Res Commun* 2002; **296**: 214–20.
15 Kullander K, Klein R. Mechanisms and functions of Eph and ephrin signalling. *Nat Rev Mol Cell Biol* 2002; **3**: 475–86.
16 Flanagan JG, Vanderhaeghen P. The ephrins and Eph receptors in neural development. *Annu Rev Neurosci* 1998; **21**: 309–45.
17 Schlessinger J, Ullrich A. Growth factor signaling by receptor tyrosine kinases. *Neuron* 1992; **9**: 383–91.
18 Kataoka H, Tanaka M, Kanamori M, Yoshii S, Ihara M, Wang YJ, Song JP, Li ZY, Arai H, Otsuki Y, Kobayashi T, Konno H, Hanai H, Sugimura H. Expression profile of EFNB1, EFNB2, two ligands of EPHB2 in human gastric cancer. *J Cancer Res Clin Oncol* 2002; **128**: 343–8.
19 Kiyokawa E, Takai S, Tanaka M, Iwase T, Suzuki M, Xiang YY, Naito Y, Yamada K, Sugimura H, Kino I. Overexpression of ERK, an EPH family receptor protein tyrosine kinase, in various human tumors. *Cancer Res* 1994; **54**: 3645–50.
20 Easty DJ, Bennett DC. Protein tyrosine kinases in malignant melanoma. *Melanoma Res* 2000; **10**: 401–11.
21 Kinch MS, Moore MB, Harpole DH Jr. Predictive value of the EphA2 receptor tyrosine kinase in lung cancer recurrence and survival. *Clin Cancer Res* 2003; **9**: 613–18.
22 D'Amico TA, Aloia TA, Moore MB, Conlon DH, Herndon JE 2nd, Kinch MS, Harpole DH Jr. Predicting the sites of metastases from lung cancer using molecular biologic markers. *Ann Thorac Surg* 2001; **72**: 1144–8.
23 Walker-Daniels J, Coffman K, Azimi M, Rhim JS, Bostwick DG, Snyder P, Kerns BJ, Waters DJ, Kinch MS. Overexpression of the EphA2 tyrosine kinase in prostate cancer. *Prostate* 1999; **41**: 275–80.
24 Walker-Daniels J, Hess AR, Hendrix MJ, Kinch MS. Differential regulation of EphA2 in normal and malignant cells. *Am J Pathol* 2003; **162**: 1037–42.
25 Zeng G, Hu Z, Kinch MS, Pan CX, Flockhart DA, Kao C, Gardner TA, Zhang S, Li L, Baldridge LA, Koch MO, Ulbright TM, Eble JN, Cheng L. High-level expression of EphA2 receptor tyrosine kinase in prostatic intraepithelial neoplasia. *Am J Pathol* 2003; **163**: 2271–6.
26 Tatsumi T, Herrem CJ, Olson WC, Tatsumi T, Herrem CJ, Olson WC, Finke JH, Bukowski RM, Kinch MS, Ranieri E, Storkus WJ. Disease stage variation in CD4+ and CD8+ T-cell reactivity to the receptor tyrosine kinase EphA2 in patients with renal cell carcinoma. *Cancer Res* 2003; **63**: 4481–9.
27 Saito T, Masuda N, Miyazaki T, Saito T, Masuda N, Miyazaki T, Kanoh K, Suzuki H, Shimura T, Asao T, Kuwano H. Expression of EphA2 and E-cadherin in colorectal cancer: correlation with cancer metastasis. *Oncol Rep* 2004; **11**: 605–11.
28 Duxbury MS, Ito H, Zinner MJ, Ashley SW, Whang EE. EphA2: a determinant of malignant cellular behavior and a potential therapeutic target in pancreatic adenocarcinoma. *Oncogene* 2004; **23**: 1448–56.
29 Duxbury MS, Ito H, Zinner MJ, Ashley SW, Whang EE. Ligation of EphA2 by Ephrin A1-Fc inhibits pancreatic adenocarcinoma cellular invasiveness. *Biochem Biophys Res Commun* 2004; **320**: 1096–102.
30 Miao H, Wei BR, Peehl DM, Li Q, Alexandrou T, Schelling JR, Rhim JS, Sedor JR, Burnett E, Wang B. Activation of EphA receptor tyrosine kinase inhibits the Ras/MAPK pathway. *Nat Cell Biol* 2001; 3: 527–30.
31 Carles-Kinch K, Kilpatrick KE, Stewart JC, Kinch MS. Antibody targeting of the EphA2 tyrosine kinase inhibits malignant cell behavior. *Cancer Res* 2002; **62**: 2840–7.
32 Walker-Daniels J, Riese DJ, 2nd, Kinch MS. c-Cbl-dependent EphA2 protein degradation is induced by ligand binding. *Mol Cancer Res* 2002; **1**: 79–87.

Oncogene (2005) 24, 5637–5647

www.nature.com/onc

# Downregulation of EphA7 by hypermethylation in colorectal cancer

Jiandong Wang[1], Hideki Kataoka[1,2], Masaya Suzuki[1], Naomi Sato[3], Ritsuko Nakamura[1], Hong Tao[1], Keiji Maruyama[4], Jun Isogaki[4], Shigeru Kanaoka[2], Megumi Ihara[1], Masamitsu Tanaka[1,7], Masao Kanamori[5,6], Toshio Nakamura[4], Kazuya Shinmura[1] and Haruhiko Sugimura*[,1]

[1]*Department of Pathology, Hamamatsu University School of Medicine, 1-20-1, Handayama, Hamamatsu 431-3192, Japan;*
[2]*Department of Medicine, Hamamatsu University School of Medicine, 1-20-1, Handayama, Hamamatsu 431-3192, Japan;*
[3]*Department of Clinical Nursing, Hamamatsu University School of Medicine, 1-20-1, Handayama, Hamamatsu 431-3192, Japan;*
[4]*Department of Surgery, Hamamatsu University School of Medicine, 1-20-1, Handayama, Hamamatsu 431-3192, Japan;*
[5]*Department of Public Health of Hamamatsu University School of Medicine, 1-20-1, Handayama, Hamamatsu 431-3192, Japan;*
[6]*Department of Lifelong Sport, Biwako Seikei Sport College, 1204 Shigachou, Shigagun, Shiga 520-0503, Japan*

**A significant reduction of EphA7 expression in human colorectal cancers was shown using semiquantitative reverse transcription–polymerase chain reaction analysis in 59 colorectal cancer tissues, compared to corresponding normal mucosas ($P=0.008$), and five colon cancer cell lines. To investigate the mechanism of EphA7 downregulation in colorectal cancer, we examined the methylation status of the 5′CpG island around the translation start site in five colon cancer cell lines using restriction enzymes, methylation-specific PCR, and bisulfite sequencing and found evidence of aberrant methylation. The expression of EphA7 in colon cancer cell lines was restored after treatment with 5-aza-2′-deoxycytidine. Analysis of methylation status in totally 75 tumors compared to clinicopathological parameters revealed that hypermethylation of colorectal cancers was more frequent in male than in female ($P=0.0078$), and in moderately differentiated than in well-differentiated adenocarcinomas ($P=0.0361$). There was a tendency that hypermethylation in rectal cancers was more frequent than in colon cancers ($P=0.0816$). Hypermethylation was also observed in colorectal adenomas. This is the first report describing the downregulation of an Eph family gene in a solid tumor via aberrant 5′CpG island methylation. It provides the evidence that EphA7 gene is involved in human colorectal carcinogenesis.**
*Oncogene* (2005) **24**, 5637–5647. doi:10.1038/sj.onc.1208720; published online 11 July 2005

**Keywords:** EphA7; colorectal cancer; DNA methylation

## Introduction

The Eph family, named for its expression in an *e*rythropoietin-*p*roducing human *h*epatocellular carcinoma cell line (Hirai *et al.*, 1987), is the largest subfamily of tyrosine kinase receptors and includes at least 14 distinct receptors and eight distinct ligands. Eph receptors have been divided into two groups based on the nature of their corresponding ligands and their sequence homology: EphA and EphB receptors (Eph Nomenclature Committee, 1997). The ligands for the Eph receptors are the ephrins: the ephrinA subclass is linked to the membrane through a GPI linkage, while the ephrinB subclass is a transmembrane protein. Ephrins and Ephs are essential for embryonic development (Chin-Sang *et al.*, 1999, 2002; Frisen *et al.*, 1999) and for the differentiation of the nervous and vascular systems (Friedman and O'Leary, 1996; Adams, 2002). They also play a role in angiogenesis (Favre *et al.*, 2003; Sullivan and Bicknell, 2003). In recent years, some of the Eph genes have been found to be overexpressed in human tumors, including neuroblastoma (Tang *et al.*, 1999), lung carcinoma (Tang *et al.*, 1999), gastric cancer (Kiyokawa *et al.*, 1994; Kataoka *et al.*, 2002), esophageal cancer (Miyazaki *et al.*, 2003), breast cancer (Wu *et al.*, 2004), and colorectal cancer (Stephenson *et al.*, 2001; Liu *et al.*, 2002, 2004; Kataoka *et al.*, 2004). Among the Eph family genes, relatively less attention has been directed toward EphA7 in human tumors, and the potential role of EphA7 in human oncology has not been addressed. Recently, we noticed a loss of expression of EphA7 during an investigation on alterations in the expression of Eph family genes in human digestive cancers (Kataoka *et al.*, 2002, 2004). EphA7, previously known as Mdk1, Hek11, Ehk-3, Ebk, and Cek11, was originally isolated from adult mouse brain (Ciossek *et al.*, 1995; Valenzuela *et al.*, 1995). EphA7 has the same major structural features as the other members of the Eph family, including a cysteine-rich region and tandem fibronectin type-III domains in its extracellular portion. In mice, EphA7 is expressed not only in its conventional full-length version, containing the intracellular tyrosine kinase domain but also in a truncated form that lacks this domain (Ciossek *et al.*, 1995; Valenzuela *et al.*, 1995). So far, the possible role of EphA7 in human colorectal cancer has not been investigated, although the overexpression of EphB4, EphA2, and Ephrin B2 has been documented in human

*Correspondence: H Sugimura; E-mail: hsugimur@hama-med.ac.jp
[7]Current address: Growth Factor Division, National Cancer Center Research Institute, 5-1-1, Tsukiji, Chuo-ku, Tokyo 104-0054, Japan
Received 30 July 2004; revised 11 March 2005; accepted 21 March 2005; published online 11 July 2005

colorectal cancer. In this study, we used semiquantitative reverse transcription–polymerase chain reaction (RT–PCR) to conduct an EphA7 expression analysis in human colorectal cancer tissues.

Since we found that the expression of EphA7 was significantly downregulated in 29 out of 59 (49%, tumor: normal mucosa ratio $<0.5$) colorectal cancer tissues, compared to normal mucosa samples, we further analysed the possible mechanism of the downregulation of EphA7 in human colorectal cancer. In the present report, we describe the methylation of 5′CpG islands in the region around the EphA7 translation start site in colorectal cell lines and in a considerable portion of primary colorectal cancers, and its clinicopathological significance in totally 75 cases of colorectal cancers.

## Results

### *Loss of EphA7 expression in primary colorectal cancers and colon cancer cell lines*

Using semiquantitative RT–PCR, we examined the expression of EphA7 in 59 primary colorectal cancer cases, five colon cancer cell lines, and some other cancer cell lines. EphA7 was significantly downregulated in 29 out of 59 (49%, tumor: normal mucosa ratio $<0.5$) of the colorectal cancer tissues, compared to expression level in paired normal mucosa samples (Figure 1). A statistical analysis (SPSS Japan Inc., Tokyo, Japan) revealed that EphA7 was significantly downregulated in colorectal cancers, compared to corresponding normal tissues ($P=0.008$). The expression of EphA7 was detected by RT–PCR in the colon cancer cell line SW480, while the loss of EphA7 expression was observed in the DLD1, HT29, HCT116, and SW620 cell lines (Figure 2). The expression of EphA7 in several other cancer cell lines of different tissue origins varied (data not shown). Quantitative real time RT–PCR was also carried out in 12 of these 59 cases. The protocol was the same as that we previously reported (Tao *et al.*, 2004). We got the consistent results to semiquantitative RT–PCR using isotope (data not shown).

We analysed various clinicopathological parameters of the cases in relation to the downregulated status of EphA7. Since some methylations are believed to relate

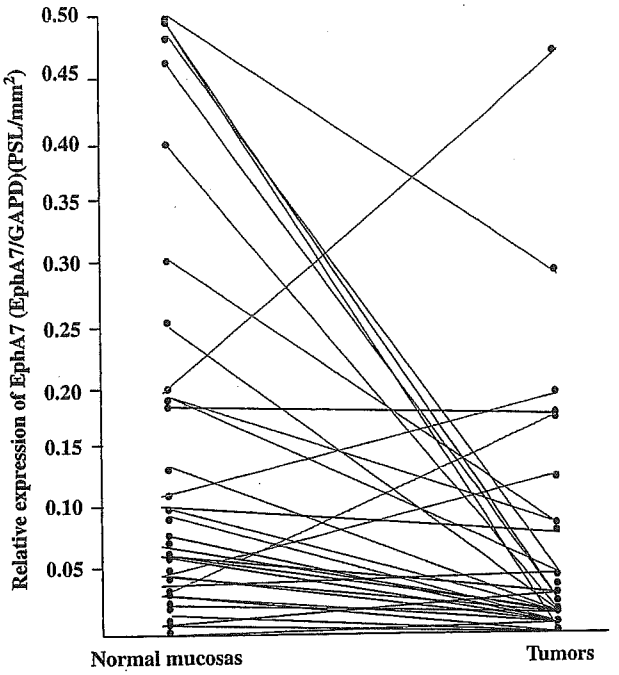


**Figure 1** EphA7 mRNA expression in primary colorectal cancer tissues (normal mucosas and tumor samples). Semiquantitative RT–PCR using $^{32}$P-labeled dCTP was carried out to determine the expression of EphA7 mRNA. The mRNA of glyceraldehyde-3-phosphate dehydrogenase (GAPDH) was also detected as a control for the integrity of the RNA samples as well as an internal control. The gel was dried and subjected to autoradiography and image analysis. The expression level (radiation dose unit PSL) was measured using a Fujix BAS1000 (MacBAS; Fuji Film, Tokyo, Japan). All RI (radio-isotope) count values, including those for GAPDH, were transformed using a logarithm. The relative expression of EphA7 in the paired tumor and normal mucosa samples from 59 colorectal cancer patients were then studied

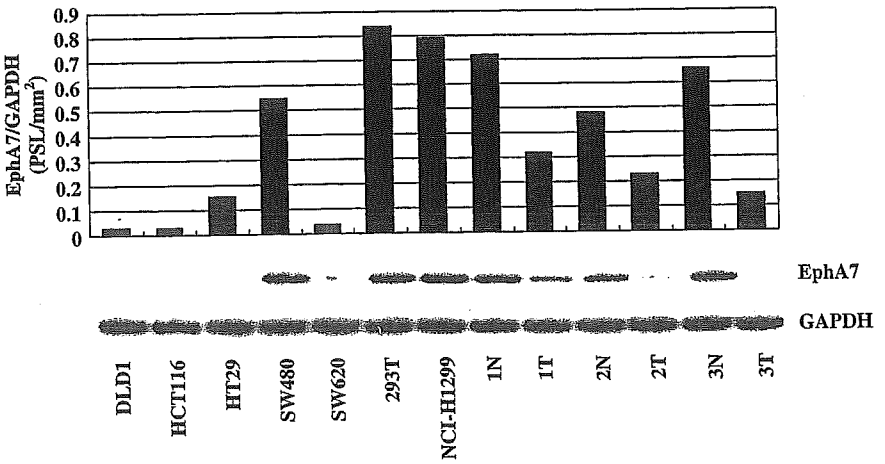


**Figure 2** Semiquantitative RT–PCR in cell lines and primary colorectal cancers. 293T (human embryo kidney cell line) and NCI-H1299 (lung cancer cell line) were used as positive controls. Cases 1, 2, and 3, consisting of both normal (N) and tumor (T) sample, are examples of the downregulation of EphA7 mRNAs in primary colorectal cancers

to aging, we examined the ages and downregulation statuses of tumors as well as the expression of EphA7 in normal mucosas. No correlation between the downregulation of EphA7 and patient age was seen. As shown in Table 1, we analysed the sex, age, locations, depth of the colorectal wall, pathological classification, clinical stage, and lymphatic metastases according to the Japanese Classification System (general rules for clinical and pathological studies on cancers of the colon, rectum and anus, Japanese Society for Cancer of the Colon and Rectum, 1998), and Dukes classification. There was no detectable significant difference between EphA7 expression and clinicopathological parameters in this data set.

**Table 1** Correlation between EphA7 expression and clinicopathologic parameters

| | *Case number* | *Average of log T/N* | *Standard deviation of log T/N* | P-*value* |
|---|---|---|---|---|
| Overall | 59 | −0.287 | 0.71 | — |
| *Sex* | | | | |
| Male | 32 | −0.199 | 0.665 | 0.297[a] |
| Female | 27 | −0.392 | 0.744 | |
| *Age* | | | | |
| ⩽55 | 11 | −0.322 | 0.671 | 0.979[b] |
| >55 and ⩽65 | 17 | −0.294 | 0.496 | |
| >65 | 31 | −0.272 | 0.832 | |
| *Location* | | | | |
| Rectum | 22 | −0.296 | 0.609 | 0.815[b] |
| Sigmoid | 15 | −0.143 | 0.752 | |
| Ascending colon | 13 | −0.366 | 0.608 | |
| Others | 9 | −0.392 | 1.036 | |
| *Depth* | | | | |
| Ss | 26 | −0.36 | 0.788 | 0.375[b] |
| Se | 10 | −0.003 | 0.645 | |
| Sm | 3 | 0.258 | 0.387 | |
| Mp | 10 | −0.309 | 0.657 | |
| a1 | 4 | −0.121 | 0.747 | |
| a2 | 2 | −0.753 | 0.391 | |
| Si | 3 | −0.642 | 0.214 | |
| m | 1 | −1.328 | — | |
| *Pathological classification* | | | | |
| mod | 12 | −0.106 | 0.807 | 0.493[b] |
| wel | 42 | −0.291 | 0.684 | |
| por | 1 | −0.588 | — | |
| muc | 4 | −0.721 | 0.736 | |
| *Clinical stage* | | | | |
| 0 | 1 | 0.66 | — | 0.501[b] |
| 1 | 12 | −0.338 | 0.69 | |
| 2 | 20 | −0.444 | 0.757 | |
| 3 | 23 | −0.187 | 0.71 | |
| 4 | 3 | −0.128 | 0.399 | |
| *Lymphatic metastases* | | | | |
| Negative | 38 | −0.354 | 0.716 | 0.332[a] |
| Positive | 21 | −0.166 | 0.698 | |
| *Dukes* | | | | |
| A | 13 | −0.261 | 0.716 | 0.718[b] |
| B | 23 | −0.38 | 0.752 | |
| C | 23 | −0.21 | 0.684 | |

—: not apply. SAS 9.1 was used. [a]Aspin Welch's *t*-test was performed. [b]ANOVA was performed. Aspin Welch's *t*-test was used when number of compared group is 2. ANOVA was used when number of compared group is more than 3

### *Hypermethylation of 5′CpG islands leads to EphA7 silencing*

There are genetic and epigenetic reasons for the loss of expression of certain genes. We screened the colon cancer cell lines and other cell lines for EphA7 genomic mutations using a single-strand conformation polymorphism (SSCP) analysis. No mutations were found in any of the colon cancer cell lines that lacked EphA7 expression. We therefore assumed that the downregulation of EphA7 in colorectal cancer was due to an epigenetic alteration. First of all, to determine whether methylation was responsible for the loss of EphA7 in colorectal cancer, we treated three colon cancer cell lines (DLD1, HCT116, and SW620) that lacked EphA7 expression with the demethylation reagent 5-aza-2′-deoxycytidine for 2 or 5 days. EphA7 mRNA expression was detected by RT–PCR in all three cell lines after the treatment. The restored expression level varied in the different cell lines and was time-dependent (Figure 3). Next, we postulated that 5′CpG islands in the area from −605 to 515 bp (from translation start site) (Figure 6a) may be hypermethylated; this area is close to the basic promoter of EphA3, another member of the EphA gene family, which has been previously characterized (Dottori *et al*., 1999). EphA7 showed a 56.1% mRNA homology to EphA3. We next used three methods to detect the methylation status of the 5′CpG islands in this area.

The methylation status of the 5′CpG islands was first determined by digestion with the methylation-sensitive and nonsensitive restriction enzymes *Hpa*II and *Msp*I, respectively, followed by PCR in five colon cancer cell lines (DLD1, HCT116, HT29, SW480, and SW620). No PCR bands were detected in all five colorectal cancer cell lines after *Msp*I digestion, while PCR bands were seen in DLD1, HCT116, HT29, and SW620 after *Hpa*II digestion. However, a PCR band was not observed in SW480 after *Hpa*II digestion. These data indicate that the 5′CG at the enzyme-recognized sites (5′CCGG) are methylated in DLD1, HCT116, HT29, and SW620, but not in SW480 (Figure 4a). The methylation status of 30 CpGs from −578 to −158 bp (from translation start site) was analysed in five colon cancer cell lines by cloning the PCR products to pGEM-T Easy vector (Promega). The hypermethylation of 5′CpG island was confirmed in these five colon cancer cell lines (Figure 5, Supplementary Figure 1). The methylation status of these 30 CpGs was also analysed in a normal musosa from colorectal patient in which the EphA7 expression was downregulated (ratio of expression EphA7 in tumor to normal was 0.043). The results showed that all 30 CpG sites were unmethylated in normal mucosa (Supplementary Figure 2) Next, we determined the methylation status in the region from −605 to 515,

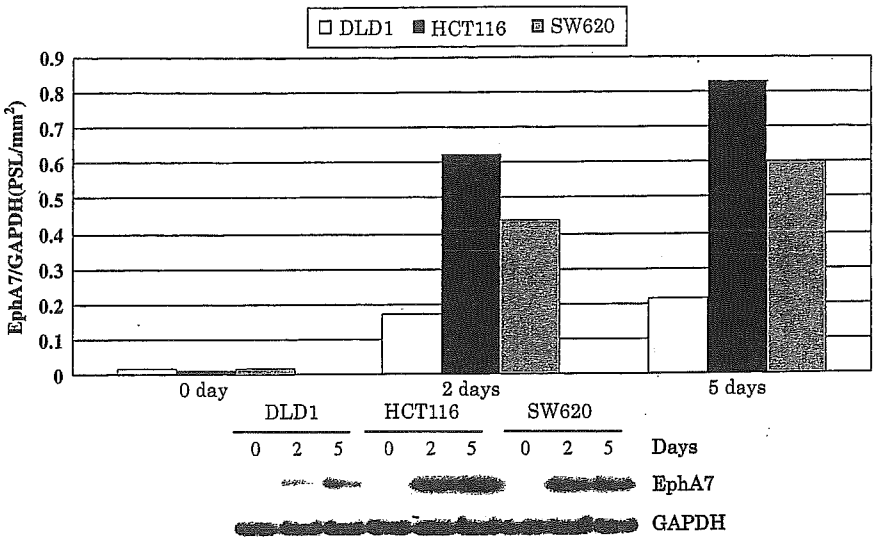


**Figure 3** The expression of EphA7 gene was restored in the DLD1, HCT116 and SW620 colon cancer cell lines after treatment with the methylation inhibitor 5-aza-2′-deoxycytidine. The cell lines were treated with 5-aza-2′-deoxycytidine for 2 or 5 days. Total RNA was harvested before (0 days) and after treatment (2 and 5 days). Semiquantitative RT–PCR was carried out to evaluate the expression of EphA7 mRNA. EphA7 expression was recovered in all three tested colon cancer cell lines by treatment with 5-aza-2′-deoxycytidine

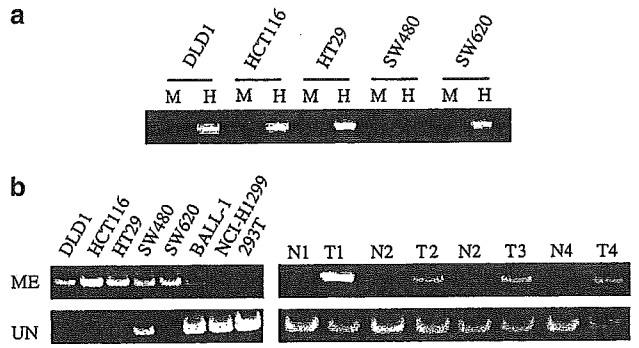


**Figure 4** (**a**) The methylation status of the 5′CpG islands upstream of the translation start site in the DLD1, HCT116, HT29, SW480, and SW620 colon cancer cell lines was determined by digestion with methylation-sensitive restriction enzymes, followed by PCR. In total, 1 $\mu$g of DNA from the colon cancer cell lines was digested with either *Msp*I (M) or *Hpa*II (H), followed by PCR amplification. (**b**) MSP analysis of the colon cancer cell lines (DLD1, HCT116, HT29, SW480, SW620), four examples of primary colorectal cancers, one lymphoma cell line (BALL-1), one lung cancer cell line (NCI-H1299) and one human embryonic kidney cell line (293T). PCR was carried out to detect methylated (ME) and unmethylated DNA (UN) using primer sets designed for methylated and unmethylated DNA, respectively

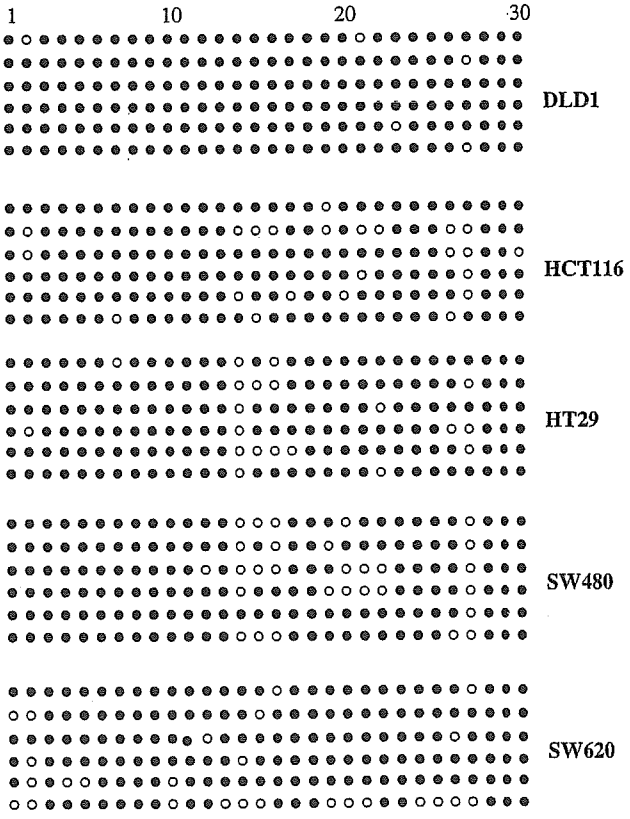


**Figure 5** Hypermethylation of 30 of 5′CpG sites between −578 to −208, relative to the translation start site, in five colon caner cell lines were examined by cloning. Cell line DNAs were bisulfite treated and amplified by PCR. The PCR products were cloned into pGEM-T Easy vector (Promega), and 12 clones were sequenced. The sequencing results of six clones from five colon caner cell lines were shown. Methylated and unmethylated alleles are shown as solid and open circles. The number of CpG sites is same as that shown in Figure 6

which is related to the translation start site and includes 80 of the 5′CG sites in the five colon cancer cell lines, one human embryonic kidney cell line (293T) and one lung cancer cell line (NCI-H1299) (expression level of EphA7 is high in 293T and NCI-H1299), as shown by direct bisulfite-sequencing. Hypermethylation was found in all of the tested cancer cell lines. The 5′CpG sites in the CpG islands can be divided into two groups: an upstream group (from 1 to 30 CpGs) and a downstream group (from 41 to 80 CpGs). Comparing expression of

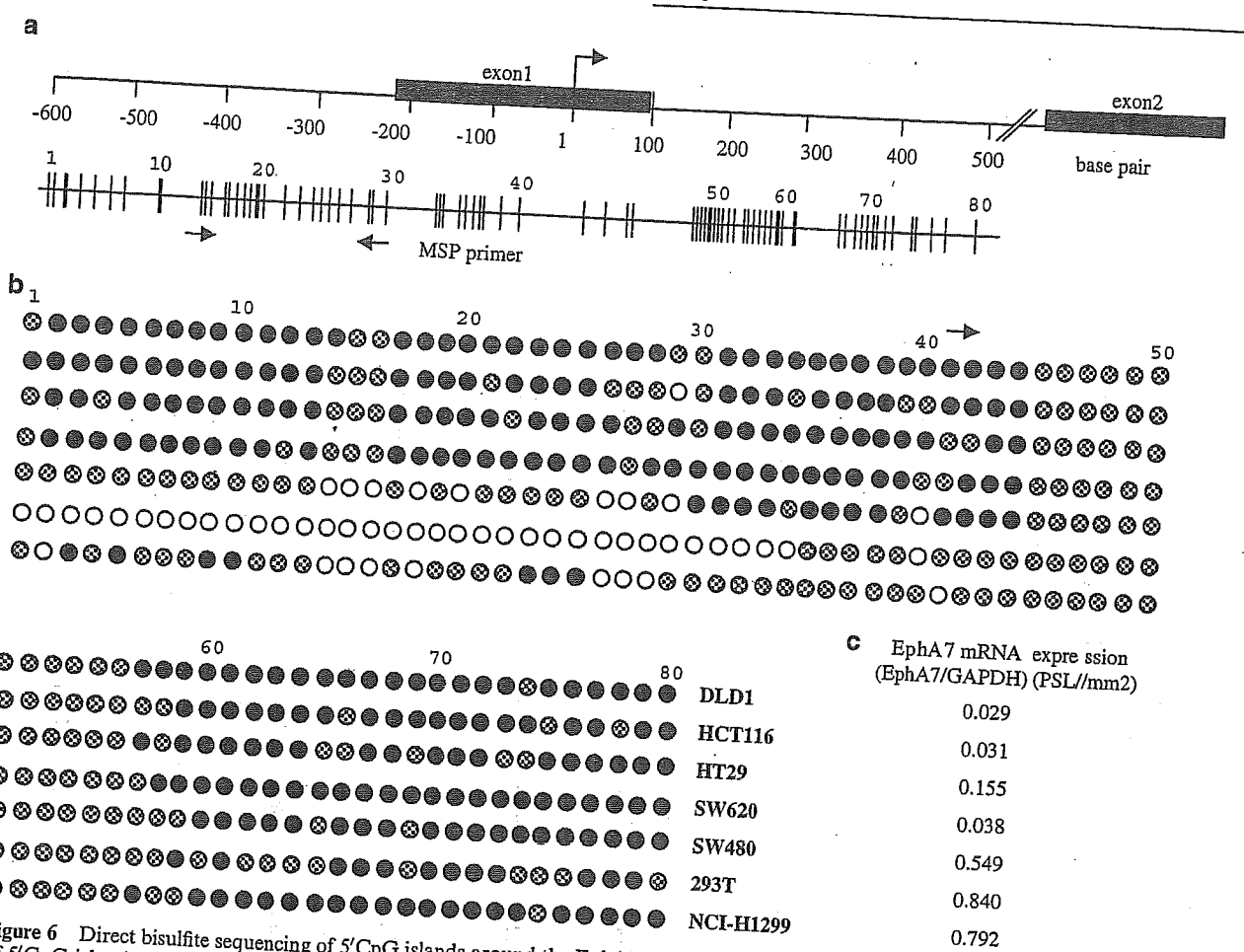


**Figure 6** Direct bisulfite sequencing of 5′CpG islands around the EphA7 translation start site. (**a**) Genomic structure and localization of 5′CpG islands around the translation start site of EphA7. The 5′CpG sites are indicated by the vertical bars. The location of MSP primer set was shown by arrows. (**b**) The methylation status of 80 CpG sites from −605 to 515 around the translation start site was analysed using direct bisulfite sequencing. PCR products from bisulfite-treated genomic DNA in five colon cancer cell lines, one embryonic renal cell line (293T) and one lung cancer cell line (NCI-H1299) were subjected to bisulfite sequencing. Methylated and unmethylated CpG sites were shown as solid (●) and open circles (○), respectively, and incompletely methylated alleles were shown as meshed cycles (⊗). (**c**) EphA7 mRNA expression in corresponding cell lines detected by semiquantitative RT–PCR. The EphA7 expression level is shown by the EphA7/GAPDH (PSL/mm²) ratio

EphA7 in the five colon cancer cell lines, 293T and NCI-H1299 (Figure 6c), the CpG methylation status of the upstream group was found to strongly relate to the expression of EphA7 (Figure 6). Finally, the genomic DNAs of five colon cancer cell lines (DLD1, HCT116, HT29, SW480, and SW620) were subjected to bisulfite modification, followed by methylation-specific PCR (MSP) (Figure 4b). Methylated DNA was detected in all of the above five colon cancer cell lines. Unmethylated DNA was strongly detected in SW480 and very weakly detected in HT29.

*Hypermethylation of 5′CpG island in tumors related to sex, pathological classification, and location of tumors*

In 13 primary colorectal cancers that EphA7 expression was downregulated, methylated DNA was detected in 12 tumors and weekly detected in four normal mucosas. In four cases that EphA7 was not downregulated, methylated DNA was weakly detected in one case of both tumor and normal mucosa (Table 2). Then MSP was used for further extensive study. In order to analyse the clinicopathological significance of hypermethylation of 5′CpG island in EphA7, we carried out MSP to 75 primary colorectal cancers. In the 75 primary colorectal cancers, (A) there were 37 cases that methylated DNAs only detected in tumors, not detected in matched normal mucosas; (B) 32 cases that methylated DNAs were not detected both in tumors and matched normal mucosas; (C) methylated DNAs were detected both in tumors and matched normal mucosas in six cases. Unmethylated DNAs were detected in all normal mucosas, and most of

**Table 2** The correlation between methylation status and EphA7 expression in primary colorectal cancers

| *EphA7 expression* | *Case number* | *Tumor* | | *Normal* | |
|---|---|---|---|---|---|
| | | *M* | *U* | *M* | *U* |
| Downregulated cases | 13 | 12 | 13 | 4 | 13 |
| Not downregulated cases | 4 | 1 | 4 | 1 | 4 |

Table 3 Relation between clinicopathologic parameters and MSP

| | *Case number* | *A* | *%* | *B* | *%* | *C* | *%* | P-*value* |
|---|---|---|---|---|---|---|---|---|
| Total number | 75 | 37 | 49 | 32 | 43 | 6 | 8 | — |
| *Sex* | | | | | | | | |
| Male | 36 | 23 | 64 | 13 | 36 | 0 | 0 | 0.0078 |
| Female | 39 | 14 | 36 | 19 | 49 | 6 | 15 | |
| *Age* | | | | | | | | |
| ⩽55 | 8 | 4 | 50 | 4 | 50 | 0 | 0 | 0.8067 |
| >55 and ⩽65 | 16 | 10 | 63 | 5 | 31 | 1 | 6.3 | |
| >65 | 51 | 23 | 45 | 23 | 45 | 5 | 9.8 | |
| *Location* | | | | | | | | |
| Ascending colon | 15 | 6 | 40 | 8 | 53 | 1 | 6.7 | |
| Cecum | 5 | 2 | 40 | 2 | 40 | 1 | 20 | |
| Descending colon | 4 | 1 | 25 | 3 | 75 | 0 | 0 | |
| Rectum | 31 | 20 | 65 | 10 | 32 | 1 | 3.2 | 0.2219 |
| Sigmoid colon | 15 | 7 | 47 | 6 | 40 | 2 | 13 | |
| Transverse colon | 5 | 1 | 20 | 3 | 60 | 1 | 20 | |
| *Pathological classification* | | | | | | | | |
| Well differentiated | 52 | 21 | 40 | 25 | 48 | 6 | 12 | |
| Moderately differentiated | 21 | 15 | 71 | 6 | 29 | 0 | 0 | 0.0867 |
| Mucinous | 2 | 1 | 50 | 1 | 50 | 0 | 0 | |
| *Lymphatic metastases* | | | | | | | | |
| Positive | 33 | 16 | 48 | 16 | 48 | 1 | 3 | 0.3391 |
| Negative | 42 | 21 | 50 | 16 | 38 | 5 | 12 | |
| *Dukes classification* | | | | | | | | |
| A | 12 | 4 | 33 | 7 | 58 | 1 | 8.3 | |
| B | 29 | 17 | 59 | 8 | 28 | 4 | 14 | 0.1598 |
| C | 34 | 16 | 47 | 17 | 50 | 1 | 2.9 | |
| *Depth* | | | | | | | | |
| a1 | 5 | 3 | 60 | 2 | 40 | 0 | 0 | |
| a2 | 7 | 5 | 71 | 2 | 29 | | 0 | |
| Sm | 6 | 3 | 50 | 3 | 50 | 0 | 0 | |
| Mp | 13 | 6 | 46 | 6 | 46 | 1 | 7.7 | 0.8314 |
| Ss | 31 | 16 | 52 | 12 | 39 | 3 | 9.7 | |
| Se | 10 | 4 | 40 | 4 | 40 | 2 | 20 | |
| Si | 3 | 0 | 0 | 3 | 100 | 0 | 0 | |
| *Bormann classification* | | | | | | | | |
| 0–1 | 10 | 6 | 60 | 4 | 40 | 0 | 0 | |
| 2 | 62 | 29 | 47 | 27 | 44 | 6 | 9.7 | 0.8686 |
| 3–4 | 3 | 2 | 67 | 1 | 33 | 0 | 0 | |
| *Ly* | | | | | | | | |
| Positive | 41 | 24 | 59 | 15 | 37 | 2 | 4.9 | 0.1571 |
| Negative | 34 | 13 | 38 | 18 | 53 | 4 | 12 | |
| *V* | | | | | | | | |
| Positive | 44 | 23 | 52 | 19 | 43 | 2 | 4.5 | 0.4387 |
| Negative | 31 | 14 | 45 | 13 | 42 | 4 | 13 | |
| *Pathological classification* | | | | | | | | |
| Well differentiated | 52 | 21 | 40 | 25 | 48 | 6 | 12 | 0.0361 |
| Moderately differentiated | 21 | 15 | 71 | 6 | 29 | 0 | 0 | |
| *Location* | | | | | | | | |
| Rectum | 31 | 20 | | 10 | | 1 | | 0.0816 |
| Not rectum | 44 | 17 | | 22 | | 5 | | |

A: methylated DNA detected only in tumor, not in normal mucosa; B: methylated DNA not detected in both tumor and normal mucosa; C: methylated DNA detected in both tumor and normal mucosa; Fisher's exact test was performed; SAS 9.1 was used

tumors. We analysed the relation between clinicopathological parameters and MSP results using SAS 9.1 soft (Table 3). In this analysis, the significant difference was shown between male and female ($P=0.0078$). The hypermethylation of EphA7 more frequently occurred in male colorectal cancer patients than in female